NEANDC (E) - 232 U Vol. V
INDC (Ger) - 24/ L + Special
FIZ-KA--4

FachInformationszentrum
Energie
Physik
Mathematik

ISSN 0172–2204
1982
Nr. 4

NEANDC (E) - 232 U Vol. V ,
(INDC (Ger) - 24/ L + Special
FIZ-KA--4)

PROGRESS REPORT ON NUCLEAR DATA RESEARCH IN THE FEDERAL REPUBLIC OF GERMANY

for the Period April 1, 1981 to March 31, 1982

August 1982

Edited by
S. Cierjacks
Kernforschungszentrum Karlsruhe
Institut für Kernphysik
and
H. Behrens
Fachinformationszentrum Energie
Physik, Mathematik, Karlsruhe

FACHINFORMATIONSZENTRUM ENERGIE · PHYSIK · MATHEMATIK GMBH KARLSRUHE

December 1982, Nr. 4 ISSN 0172–2204

Vertrieb:

Fach-
informations-
zentrum

Energie
Physik
Mathematik GmbH
Karlsruhe

7514 Eggenstein-Leopoldshafen 2
Telefon (07247) 824600/01
Telex 7826487 fize d

Preis: 12,– DM (incl. MwSt.) + Porto

Printed in the Federal Republic of Germany

Druck:
Badendruck GmbH
Lammstraße 1–5
7500 Karlsruhe 1

Foreword

This report has been prepared to promote exchange of nuclear data research information between the Federal Republic of Germany and the other member states of NEA and IAEA. It brings together progress reports from KfK Karlsruhe, KFA Jülich, the Universities of Kiel, Köln, Mainz, Marburg, München and Stuttgart, as well as from PTB Braunschweig and FIZ Karlsruhe. The emphasis in the works reported here has been on measurement, evaluation and compilation of application-oriented nuclear data, such as those relevant to fission and fusion reactor technologies, development of intense spallation neutron sources, production of medically important short-lived radioisotopes, etc.

Each contribution is presented under the laboratory heading where the work was done. If the work is relevant to requests in the World Request List for Nuclear Data, WRENDA 79/80 (INDC (SEC) - 73/URSF), the corresponding request identification numbers have been listed after the title and authors' names of the respective contribution.

Karlsruhe, August 1982

S. Cierjacks
H. Behrens

C O N T E N T S

KERNFORSCHUNGSZENTRUM KARLSRUHE
INSTITUT FÜR NEUTRONENPHYSIK UND REAKTORTECHNIK

INSTITUT FÜR CHEMIE (1): NUKLEARCHEMIE
KERNFORSCHUNGSANLAGE JÜLICH

INSTITUT FÜR REINE UND ANGEWANDTE KERNPHYSIK
UNIVERSITÄT KIEL, FORSCHUNGSREAKTOR GEESTHACHT

INSTITUT FÜR KERNCHEMIE
UNIVERSITÄT ZU KÖLN

INSTITUT FÜR KERNCHEMIE
JOHANNES GUTENBERG-UNIVERSITÄT MAINZ

INSTITUT FÜR KERNCHEMIE
PHILIPPS-UNIVERSITÄT MARBURG

REAKTORSTATION GARCHING; FACHBEREICH PHYSIK
TECHNISCHE UNIVERSITÄT MÜNCHEN

INSTITUT FÜR KERNENERGETIK UND ENERGIESYSTEME (IKE)
UNIVERSITÄT STUTTGART

INSTITUT FÜR STRAHLENPHYSIK
UNIVERSITÄT STUTTGART

PHYSIKALISCH-TECHNISCHE BUNDESANSTALT
BRAUNSCHWEIG

KERNFORSCHUNGSZENTRUM KARLSRUHE
INSTITUT FÜR ANGEWANDTE KERNPHYSIK

1. 3 MV Van de Graaff-Accelerator

1.1 The Capture Cross Sections of the Neon Isotopes and the s-Process Neutron Balance*

J. Almeida

The neutron capture cross sections of the three stable neon isotopes have been measured by the time-of-flight method in the energy range from 5 to 200 keV, using hydrogen free fast liquid scintillator detectors and the Maier-Leibnitz pulse height weighting technique. The sensitivity of the experimental set-up has been increased by about 50 % through improvements in the high pressure samples, neutron collimation, and shielding. The data analysis has been refined, especially with respect to the crucial problem of background elimination. This allowed the 30 keV Maxwell averaged cross sections to be determined with an accuracy of better than 1 mb. The total cross sections, which are needed for the background correction in the capture measurements, were also measured between 5 and 800 keV.

The results have been used to discuss neutron balance and temperature during s-process nucleosynthesis.

---

*KfK-Report 3347, Kernforschungszentrum Karlsruhe (1982)

1.2 Neutron Capture Width of s-Wave Resonances in ^{56}Fe, ^{58,60}Ni and ^{27}Al*

K. Wisshak, F. Käppeler, G. Reffo[+], and F. Fabbri[+]

(Relevant to request numbers: 762074, 692101, 692103, 692104, 714005, 741040, 753036, 762100, 792201, 792202, 761039, 692128, 692131, 702009, 741053, 753039, 762110, 792207, 792208, 792010, 741056, 741059)

The neutron capture widths of s-wave resonances in ^{56}Fe(27.7 keV) ^{58}Ni (15.4 keV), ^{60}Ni (12.5 keV) and ^{27}Al (35.3 keV) have been determined, using a set-up completely different from LINAC experiments. A pulsed 3 MV Van de Graaff accelerator and the ^{7}Li(p,n) reaction served as a

neutron source. The proton energy was adjusted just above the reaction threshold to obtain a kinematically collimated neutron beam. This allowed to position the samples at a flight path as short as ∿90 mm. Capture events were detected by three Moxon-Rae detectors with graphite, bismuth-graphite and pure bismuth converter, respectively. The measurements were performed relative to a gold standard. The set-up allows to discriminate capture of scattered neutrons completely by time-of-flight and to use very thin samples (0.15 mm) in order to reduce multiple scattering. After correction for deviations of the detector efficiency from a linear increase with gamma-ray energy, the results obtained with different detectors agree within their remaining systematic uncertainty of ∿5 %. Only preliminary results are presented.

---

*Proc. of the NEANDC/NEACRP Specialists Meeting on Fast-Neutron Capture Cross Sections, Argonne, 20-23 April 1982, to be published.

+Comitato Nazionale per l'Energia Nucleare, Bologna, Italy.

1.3 Neutron Capture Resonances of ^{56,58}Fe in the Energy Range from 10 to 100 keV*

F. Käppeler, L.D. Hong, K. Wisshak, and G. Rupp

(Relevant to request numbers, 692101, 692103, 692104, 714005, 741040, 753036, 762100, 792201, 792202, 741046, 691104, 762179)

The neutron capture cross section of ^{56,58}Fe has been measured in the energy range from 10 to 250 keV. Capture gamma rays were detected by two C_6D_6 detectors and the pulse height weighting technique was applied. The samples were located at a flight path of 60 cm. The distance of 4 cm from sample to the detectors was sufficient to discriminate events due to capture of scattered neutrons by time of flight. In this way reliable results were obtained for the strong s-wave resonances, too. The measured capture yield was analyzed using the FANAC code. The energy resolution allowed to extract resonance parameters in the energy region from 10 to 100 keV. The individual systematic uncertainties are discussed in detail and a comparison to the results of other authors is made.

---

*to be submitted for publication to Nucl. Sci. Eng.

1.4 Neutron Capture Cross Section of ^{80}Kr and ^{86}Kr in the Energy Range from 4 to 290 keV

G. Walter, F. Käppeler, D. Erbe, and Z.Y. Bao[+]

We have measured the cross sections of $^{80}Kr\ (n,\gamma)^{81}Kr$ and $^{86}Kr(n,\gamma)^{87}Kr$ in an energy range from 4 to 290 keV relative to ^{197}Au. As a low lying isomeric state is known to exist in ^{81}Kr our data, by the method of measurement, represent the sum of the capture cross sections to the ground state and the isomer.

The experiment was performed by the time-of-flight (TOF) technique using a pulsed proton beam from the Karlsruhe 3.75 MV Van de Graaff-accelerator with a repetition rate of 1 MHz. Neutrons were produced by the $^{7}Li(p,n)^{7}Be$ reaction and collimated by a $^{6}Li/^{10}B$-arrangement. The samples were mounted on a sample changer and sequentially brought into the measuring position. The deexcitation gamma rays of the compound nucleus were detected by two C_6D_6 scintillators operating as Maier-Leibnitz-detectors. Coincident events were rejected from the spectra and separately recorded for later correction of multiple weighting.

We achieved an overall time resolution of 1.2 ns corresponding to an energy resolution of 200 eV at 30 keV. Monitoring of the neutron flux was performed by a ^{6}Li-glass detector at 90° to the beam axis. From the data we calculated the Maxwell-averaged cross sections at kT = 30 keV to (257 ± 13)mb for ^{80}Kr and (5.6 ± 0.7) mb for ^{86}Kr. The quoted uncertainty arises mainly from systematic errors.

[+]Institute of Atomic Energy, Peking, China

1.5 On the Origin of the Solar System Abundances of ^{113}In, ^{114}Sn, and ^{115}Sn*

R.A. Ward[+] and H. Beer

The neutron capture cross section of ^{114}Cd to the 53.30 h ground state in ^{115}Cd has been measured via neutron activation. Using this result in conjunction with the total neutron-capture rate of ^{114}Cd, the relative

population of $^{115}Cd^{o}$ (53.38 h) was found to be 0.78 ± 0.13 at an energy appropriate to 30 keV stellar neutrons. In addition, we have quantitatively examined the isomeric structure of the key nuclei: ^{113}Cd, ^{114}In, ^{115}Cd, and ^{115}In which all crucially influence the neutron-capture flows of the s-process as well as the final beta-decays of the r-process in the Cd-In-Sn region. Using temperature and free-neutron histories of various stellar s-process environments, we find that a simple combination of separate s- and r-process components can generally reproduce most of the solar abundances of ^{113}In and ^{115}Sn under typical stellar conditions. Resulting implications for various models of the p-process are also discussed.

---

*Astron. and Astrophys. 103 (1981) 189

+Lawrence Livermore National Laboratory,
Livermore, California, USA

1.6 ^{176}Lu: Cosmic Clock or Stellar Thermometer?*

H. Beer, F. Käppeler, K. Wisshak, and R.A. Ward+

We quantitatively examine the various experimental and theoretical aspects of the stellar synthesis of the long-lived ground state of ^{176}Lu (3.6×10^{10} y). We discuss the various regimes of stellar temperature and free-neutron density in which either: (i) the internal electromagnetic couplings between $^{176}Lu^{o}$ and $^{176}Lu^{m}$ (3.68 hours) are sufficiently slow that they may be treated as separate nuclei, or (ii) the internal couplings are rapidly able to establish thermal equilibrium between $^{176}Lu^{o}$ and $^{176}Lu^{m}$. Case (i) above allows $^{176}Lu^{o}$ to be used as a cosmic clock of galactic s-process nucleosynthesis. As experimental input to the cosmic clock, we have measured the 30-keV neutron capture cross sections: $\sigma(^{170}Yb)$ = 766 ± 30 mb and $\sigma(^{175}Lu)$ = 1266 ± 43 mb. This latter value also yields the branching ratio, B, to $^{176}Lu^{o}$ from neutron capture on ^{175}Lu as: B(24 keV) = 0.362 ± 0.038.

---

*Astrophysical Journal Suppl. 46 (1981) 295

+Lawrence Livermore National Laboratory,
Livermore, California, USA

1.7 ^{178,179,180}Hf and ^{180}Ta(n,γ) Cross Sections and Their Contribution to Stellar Nucleosynthesis*

H. Beer and R.L. Macklin+

The neutron capture cross sections of ^{178,179,180}Hf were measured in the energy range 2.6 keV to 2 MeV. The average capture cross sections were calculated and fitted in terms of strength functions. Resonance parameters for the observed resonances below 10 keV were determined by a shape analysis. Maxwellian averaged capture cross sections were computed for thermal energies kT between 5 and 100 keV. The cross sections for kT = 30 keV were used to determine the population probability of the 8^- isomeric level in ^{180}Hf by neutron capture as (1.24 ± 0.06) % and the r-process abundance of ^{180}Hf as 0.0290 (Si≡10^6). These quantities served to analyze s- and r-process nucleosynthesis of ^{180}Ta.

---

*To be published in Phys. Rev. C

+Oak Ridge National Laboratory, Oak Ridge, Tenn. 37830, USA

1.8 Neutron Capture Nucleosynthesis of Nature's Rarest Stable Isotope*

H. Beer and R.A. Ward+

^{180}Ta with a solar abundance of 2.46 x 10^{-6} (Si≡10^6) is nature's rarest stable isotope. Until now it was not possible to explain its origin satisfactorily by spallation which is the commonly assumed source of ^{180}Ta. This is due to insufficient knowledge of the ^{180}Ta level scheme. In the present investigation an alternative production mechanism is proposed. The ^{180}Ta abundance is explained by a small branching in the s- or post r-process neutron capture nucleosynthesis. In this picture the population of an isomeric state in ^{180}Hf^m is of crucial importance. The capture cross section of ^{179}Hf to this isomeric state has been measured as 13.5 ± 0.6 mb at 25 keV.

---

*Nature 291, 308 (1981)

+Lawrence Livermore National Laboratory, Livermore, California, USA

1.9 Fast Neutron Capture on ^{180}Hf and ^{184}W and the Solar Hafnium and Tungsten Abundance*

H. Beer, F. Käppeler and K. Wisshak

The capture cross section of ^{180}Hf and ^{184}W were measured by the activation method and via direct detection of prompt gamma-rays, respectively. The Maxwellian averaged cross sections for kT = 30 keV were used to decompose the solar isotopic Hf- and W-abundances into s- and r-process contributions. Examination of the r-process contributions provided evidence that the abundances of Hf and W might be smaller than quoted in recent abundance compilations. Therefore it is proposed to reconsider the information from meteorite analyses and to perform new measurements if necessary.

---

*Astronomy and Astrophys. 105 (1982) 270

1.10 Calculated Gamma-ray Spectra for keV Neutron Capture in ^{240}Pu, ^{242}Pu and ^{238}U*

G. Reffo[+], F. Fabbri[+], K. Wisshak, and F. Käppeler

(Relevant to request numbers 712066, 691389, 692451, 692452, 692453, 714032, 721137, 754006, 762214, 741139, 692442, 792050, 712102, 721098, 721142, 722043, 742010, 754014, 762223, 741141, 792052)

Capture gamma-ray spectra of ^{240}Pu, ^{242}Pu and ^{238}U were calculated in the framework of the spherical optical model and the statistical model. A consistent set of input parameters was determined from available experimental information or from model guided systematics. The complete gamma-ray cascades were calculated considering all possible transitions up to multiplicity 7. All experimental information on level schemes and gamma-ray transition probabilities of the compound nuclei was explicitely included as input.

The capture gamma-ray spectra were used to correct experimental data for the capture cross sections of ^{240}Pu and ^{242}Pu from a relative

measurement using a Moxon-Rae detector with graphite converter and ^{197}Au as well as ^{238}U as standards. This correction is required to take into account that the detector efficiency is not exactly proportional to the gamma-ray energy. The resulting correction factors proved to be negligible for measurements relative to ^{238}U whereas they are ∿3 % if gold is used as a standard.

---

*submitted for publ. in Nucl. Sci. Eng.

+Comitato Nazionale per l'Energia Nucleare, Bologna, Italy

1.11 The Neutron Capture Cross Section of ^{243}Am in the Energy Range from 10 to 250 keV

K. Wisshak, F. Käppeler, and G. Rupp

(Relevant to request numbers: 721101, 732104, 741128, 761100, 762028, 792147, 792237, 794005)

The capture cross section of ^{243}Am has been measured /1/ in the energy range 10-250 keV using kinematically collimated neutrons from the $^{7}Li(p,n)$ and T(p,n) reaction. The samples are positioned at flight paths of 5-7 cm and gold was used as a standard. Capture events were detected by two Moxon-Rae detectors with graphite and bismuth-graphite converters shielded by 0.5 - 2 cm of lead. Fission events were detected by a NE 213 liquid scintillator.

References

/1/ K. Wisshak, F. Käppeler, G. Reffo, and F. Fabbri, Proc. NEANDC/NEACRP Specialists Meeting on Fast-Neutron Capture Cross Sections, Argonne 20-23 April 1982, to be published.

KERNFORSCHUNGSZENTRUM KARLSRUHE
INSTITUT FÜR KERNPHYSIK

1. SIN Cyclotron

1.1 Neutron and Charged Particle Production Yields and Spectra from Thick Uranium Targets by 590 MeV Protons

S. Cierjacks, F. Raupp, Y. Hino, S.D. Howe [1], L. Buth [2], M.T. Rainbow [3], M.T. Swinhoe [4]

The investigations of depth and angular dependent yields and spectra from thick heavy metal targets were continued. The data analysis for thick uranium targets has been completed [1, 2, 3]. In Fig. 1 three typical spectra of neutrons emitted from a 10 x 10 cm^2, 40 cm long, uranium target at a laboratory angle of 90^o are shown. The three different curves belong to the yields from an average target depth of 2.5, 7.5 and 12.5 cm of protons into the target. All spectra exhibit the characteristic two-component shape attributed to evaporation and cascade neutrons (the latter of which produces the broad shoulder around $\sim$ 100 MeV). The absolute yields of evaporation neutrons for uranium are about a factor of two higher than those from an equivalent lead target. The enhanced yields for uranium are attributed to high-energy and neutron-induced fission.

1.2 Measurements of Differential Production Cross Sections for Neutrons by 590 MeV Protons

S. Cierjacks, Y. Hino, S.D. Howe [1], F. Raupp, L. Buth [2], M.T. Rainbow [3], M.T. Swinhoe [4]

Differential cross sections for neutrons emitted from thin targets of C, Al, Fe, In, Ta, Pb and U were measured at laboratory angles of 30^o, 90^o and 150^o. The measurements were performed by the time-of-flight technique using an NE 213 liquid scintillator and the microstructure pulses from the SIN cyclotron. Data analysis of the measurements is almost completed [1]. The differential cross sections for neutrons emitted from the various thin targets at a laboratory angle of 90^o are shown in Fig. 2. The two characteristic components in the cross section

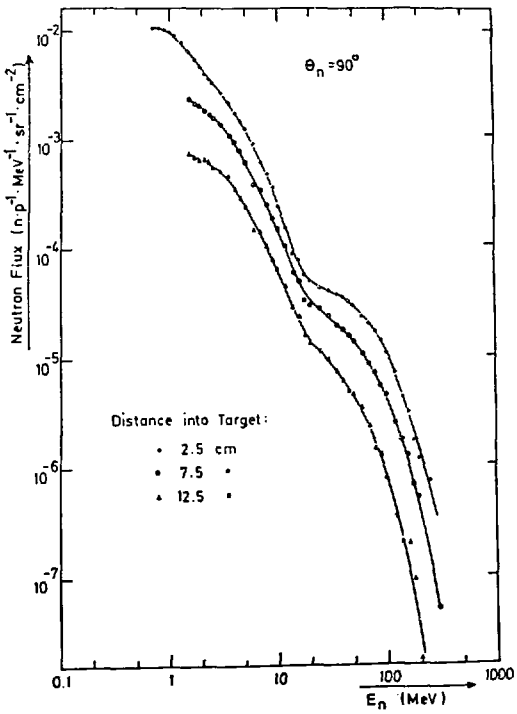

Fig. 1

Differential spectra for neutrons emitted from a thick uranium target at a laboratory angle of 90°. The three curves refer to 2.5, 7.5 and 12.5 cm average depth into target.

Fig. 2

Differential cross sections for neutrons emitted from various thin metal targets at a laboratory angle of 90°. The proton bombarding energy was 590 MeV.

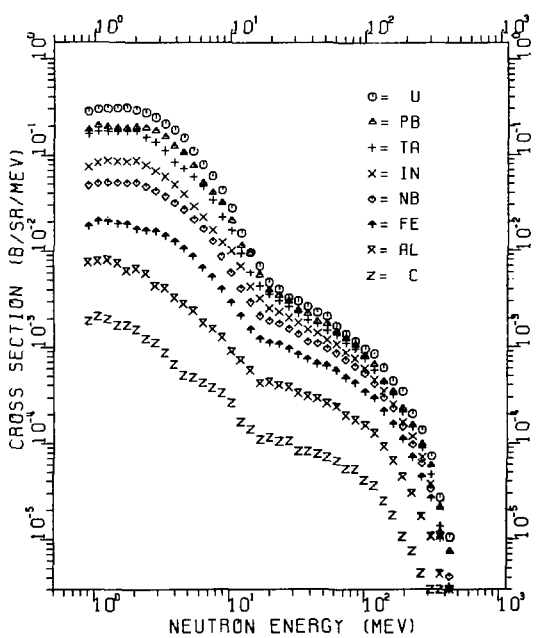

curves are attributed to evaporation neutrons (dominating the spectrum shape below ∿ 15 MeV) and cascade neutrons (determining the shape above 15 MeV). The cross sections are seen to increase smoothly which increasing target mass, and the fraction of cascade neutrons in the individual curves tends to increase with decreasing mass number. Some results of the measurements have been compared with HETC - calculations performed by Armstrong and Filges [4, 5]. First comparisons revealed a considerable degree of disagreement. A typical example is given in Fig. 3 showing the differential cross sections for lead at a laboratory angle of 90°. Calculations of the lead cross sections were made for three different choices of the level density parameter B_o, but changes in B_o effect only the evaporation energy range, and even here only small changes occur for the adopted choices . It can be seen from Fig. 3 that the calculations overpredict the measured results by about a factor of 1.5 with some inevitable changes between the calculated curves over the range from 0.5 to 15 MeV. Above 15 MeV the code underpredicts the cross sections

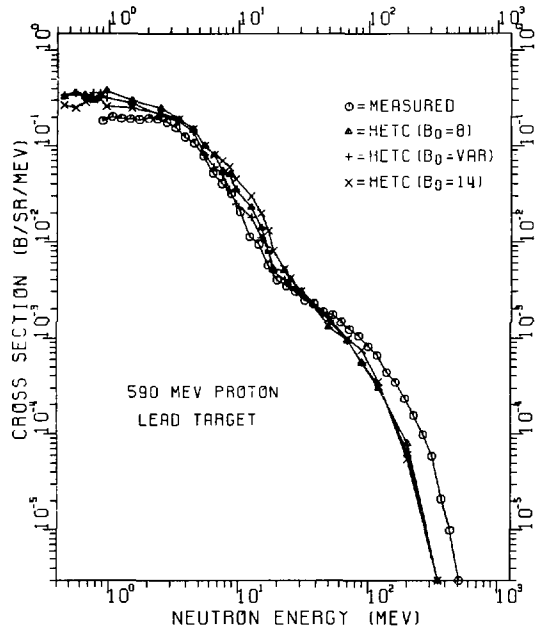

Fig. 3 Comparison of measured and calculated differential cross sections emitted from a thin lead target at a laboratory angle of 90°. Calculations were made for three different choices of the level density parameter B_o [5]

and the difference between the measured and the calculated curves increases rapidly with increasing neutron energy. It is planned to intensity comparisons of measured and calculated differential cross sections, in order to assess the discrepancies between measurements and HETC predictions more systematically.

1.3 Measurements of Differential Production Cross Sections for Charged Particles by 590 MeV Protons

S. Cierjacks, S.D. Howe [1], Y. Hino, F. Raupp, L. Buth [2], M.T. Swinhoe [4], M.T. Rainbow [3]

The differential production cross sections for charged particles produced by 590 MeV protons incident on thin samples of C, Al, Fe, In, Ta, Pb and U were measured at laboratory angles of 23°, 45°, 90°, 135° and 157°, in order to complement differential neutron data. A similar time-of-flight technique as for the neutron measurements (section 1.2) was used. Charged particle identification was accomplished by a coincidence method employing a thin plastic scintillation counter in front of the principal NE 213 detector and by consideration of specific charged-particle energy losses. The data analysis of the 90° and 157° measurements have been completed [1, 6]. This analysis provided differential data for the emission of secondary protons, deuterons, tritons and pions ($\pi^+ + \pi^-$) of energies higher than a few tens of MeV. In Fig. 4 the results obtained for secondary protons emitted from thin samples of Al, Nb, Pb and U at 90° are shown. Individual cross section curves are seen to vary smoothly with proton emission energy. Differential cross sections increase rapidly with increasing mass number. A preliminary comparison of experimental results with HETC calculations is illustrated in Fig. 5 which shows the 90° and 157° proton data for lead. While the calculations reasonably reproduce the measured shapes of the cross section curves, the code underpredicts the absolute cross sections by about a factor of three. Some comparisons of pion production cross section data have also been made, but the agreement was rather poor [4]. Comparisons of differential deuteron and triton cross sections in the measured range are presently not very attractive, because the code calculates deuteron and triton spectra only from the evaporation phase [4], the energy range of which is not covered in our measurements.

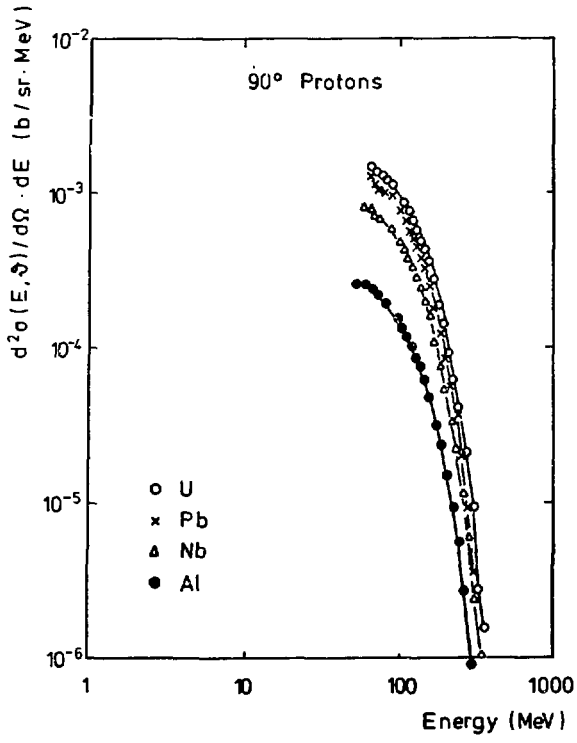

Fig. 4

Differential cross sections for secondary protons emitted from thin aluminum, niobium, lead and uranium targets at a laboratory angle of 90°. The proton bombarding energy was 590 MeV.

Fig. 5

Comparison of measured and calculated differential cross sections for secondary protons emitted from a thin lead target at laboratory angles of 90° and 157°.

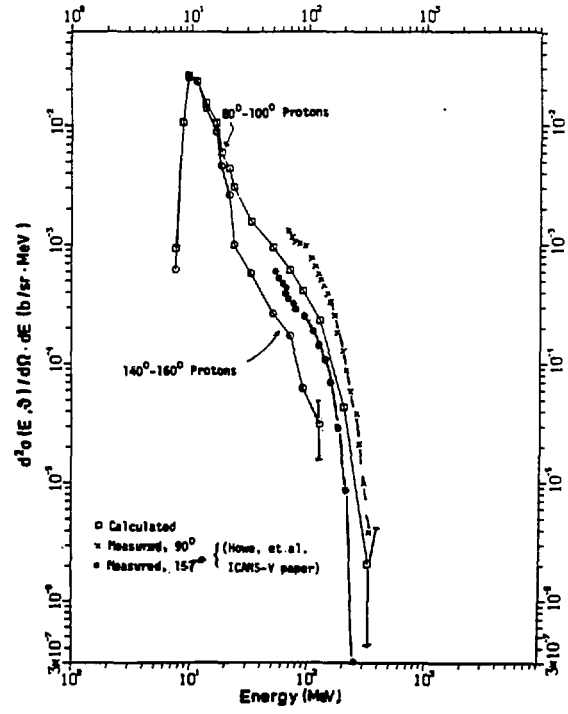

1.4 Measurement of the Absolute Detection Efficiency of an NE 213 Liquid Scintillator for Neutrons in the Energy Range 50-450 MeV

S. Cierjacks, M.T. Swinhoe [4], L. Buth [2], S.D. Howe [1], F. Raupp, H. Schmitt [5], L. Lehmann [5]

The average neutron detection efficiency of a 4.5 cm diameter, 3.0 cm thick NE 213 liquid scintillator has been measured for neutron energies between 50 and 450 MeV. The knowledge of the efficiency for this type of detector was an important prerequisite for absolute neutron measurements in the studies described in sections 1.1, 1.2, 2.1 and 2.2. Measurements were performed for three detector thresholds of 0.6, 4.2 and 17.5 MeV electron energy (MeV_{ee}) using the Freiburg University fast neutron facility at the SIN cyclotron. Employing a liquid hydrogen scatterer placed in the incident neutron beam allowed to employ the associated particle method and measuring elastically scattered neutrons and recoil protons at kinematically related angles. The results of the measurements are listed in Table I. In this table experimental results are compared with calculated efficiencies obtained with the Monte Carlo program of Stanton modified by Cecil et al. *[7]*. The good agreement between experiments and calculations shows that the

Table I

Measured and Calculated Efficiency Values for Three Thresholds.

Neutron energy (MeV)	Efficiency values (%)					
	0.6 MeV_{ee}		4.2 MeV_{ee}		17.5 MeV_{ee}	
	meas.	calc.	meas.	calc.	meas.	calc.
49.5	4.98	5.40	4.01	4.01	0.86	0.85
75.4	3.82	3.89	2.86	3.11	1.06	1.07
105	3.73	3.40	2.94	2.55	0.88	0.99
182	3.34	2.90	2.47	2.15	0.80	0.62
265	2.98	2.97	2.12	1.99	0.49	0.48
335	3.03	2.87	2.05	1.92	0.60	0.37
413	3.31	2.92	2.08	2.00	0.70	0.37

predictions from Cecil's code should also be sufficiently accurate for other than the present application. The results have been published in the open literature [8].

2. SATURNE Accelerator

2.1 Neutron and Charged Particle Production Yields and Spectra from 1100 MeV Proton Bombardment of Thick Heavy Metal Targets

S. Cierjacks, F. Raupp, S.D. Howe [1], Y. Hino, L. Buth [2], M.T. Swinhoe [4], M.T. Rainbow [3]

The previous measurements of neutron and charged particle production yields and spectra from 1100 MeV proton bombardment of thick lead and uranium targets have been analyzed [1]. The main objective of the investigations at 1100 MeV was to provide a few specific sample results for comparisons with the corresponding 600 MeV data, in order to identify significant new features (if any) at the increased proton energy. The spectral distribution of neutrons emitted at 90^{o} from an average target depth of 2.5 cm for both bombarding energies is shown in Fig. 6. Except for the higher energy limit of the spectrum and the increased yield for 1100 MeV incident protons both neutron spectra are very similar. The difference for incident proton energies of 590 and 1100 MeV is more pronounced for the spectra of secondary protons emitted at 90^{o} from thick lead targets as shown in Fig. 7. These data were also taken from an average target depth of 2.5 cm. The unexpectedly high yield of high energy protons in the 1100 MeV curve has possibly some consequences on design concepts for a cold neutron source at a 1100 MeV proton beam spallation facility.

2.2 Measurement of the High Energy Component of the Neutron Spectrum from Moderated Spallation Sources

S. Cierjacks, Y. Hino, S.D. Howe [1], F. Raupp, L. Buth [2], M.T. Swinhoe [4], M.T. Rainbow [3]

The previous spectrum measurements of high energy neutrons associated with the thermal and epithermal beams from a moderated spallation source have

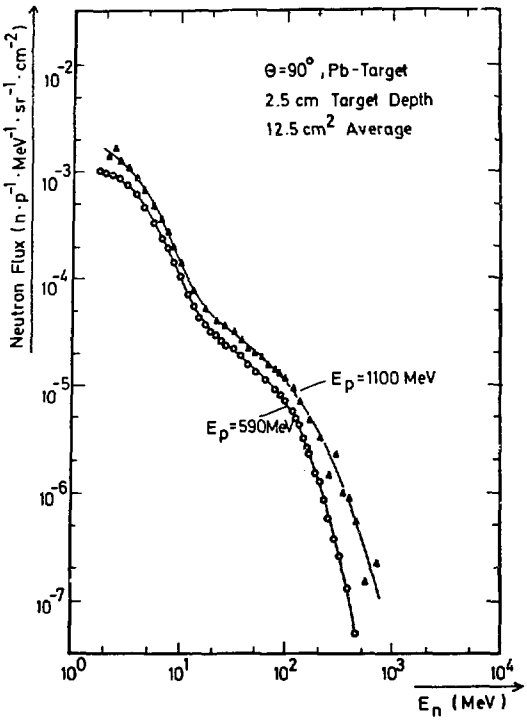

Fig. 6

Differential spectra for neutrons emitted from a thick lead target at a laboratory angle of 90°. The diagram compares the spectra from 2.5 cm depth into target for the two proton bombarding energies of 590 and 1100 MeV.

Fig. 7

Differential spectra for high energy secondary protons emitted from a thick lead target at a laboratory angle of 90°. The figure compares the spectra from 2.5 cm into target for the two proton bombarding energies of 590 and 1100 MeV.

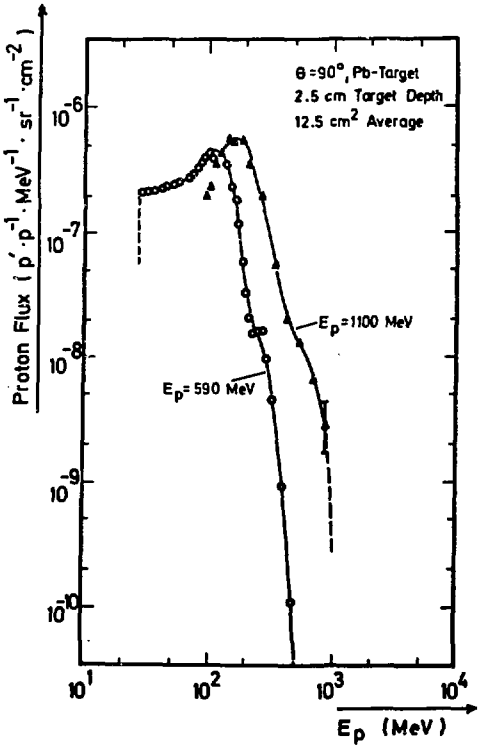

been complemented by new studies using an improved technique [9]. This technique employs a 7 cm diameter, 30 cm long NE 213 neutron detector and iterative unfolding of analog spectra by a FERDOR code [10]. The new technique allowed to derive undistorted neutron spectra over the extended energy range from ∿ 1 to 250 MeV. The neutron detector and the improved unfolding method were tested by measuring the same neutron spectrum from a bare uranium target at the SIN both by spectrum unfolding and by time-of-flight. A recent spectrum measurement using the new technique is shown in Fig. 8. This figure displays the high energy spectrum from a target configuration with a primary lead target, a polyethelene moderator and a large beryllium reflector. Data obtained with the new technique are indicated by the crosses, and the vertical lines are the uncertainties introduced by the unfolding method. Open circles show our previous results for the same target configuration measured with a small neutron detector, and using a simplified "rectangular" unfolding method. It can be seen that the old unfolding technique produced a significant spectrum distortion in the range above about ∿ 50 MeV.

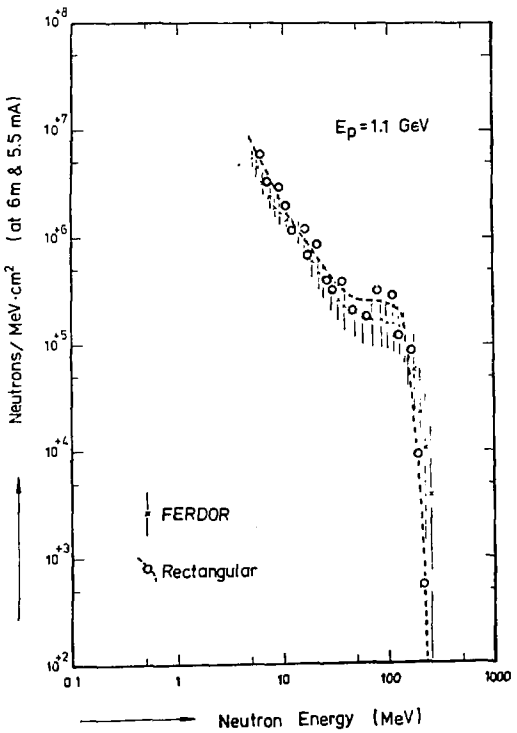

Fig. 8

High energy spectra for neutrons emitted from a shielded moderated spallation source. The target configuration bombarded by 1100 MeV protons consisted of a thick primary lead target, a polyethylene moderator in wing geometry and a large beryllium reflector. For explanation of symbols see text.

[1] Not at Los Alamos Scientific Laboratory, Los Alamos, New Mexico, USA

[2] Permanent member of the Institut für Neutronenphysik und Reaktortechnik, Kernforschungszentrum Karlsruhe

[3] Present address: Physics Division, A.A.E.C. Research Establishment, Sutherland 2232, N.S.W. Australia

[4] Now at Nuclear Physics Division, AERE Harwell, Oxfordshire, OX 11 ORA, U.K.

[5] Fakultät für Physik, Universität Freiburg, D-7800 Freiburg, Hermann-Herder-Str. 3

References

[1] S. Cierjacks, F. Raupp, S.D. Howe, Y. Hino, M.T. Swinhoe, M.T. Rainbow and L. Buth, High Energy Particle Spectra from Spallation Targets, ICANS-V, Proc. 5th Meeting of the Int. Coll. on Advanced Neutron Sources, G.S. Bauer and D. Filges (Eds.), Jül-Conf-45, p. 215-240, 1981

[2] F. Raupp, S. Cierjacks, Y. Hino, M.T. Rainbow, M.T. Swinhoe, L. Buth, Neutron Production Yields and Spectra from 590 MeV Proton Bombardment of Thick Uranium Targets, ICANS-V, Proc. 5th Meeting of the Int. Coll. on Advanced Neutron Sources, G.S. Bauer and D. Filges (Eds.), Jül-Conf-45, p. 333-342, 1981

[3] F. Raupp, Messung der orts- und winkelabhängigen Spektren schneller Neutronen und geladener Sekundärteilchen aus Spallationsreaktionen von 590 MeV Protonen in dicken Urantargets, Diplom Thesis, University Karlsruhe, 1982

[4] T.W. Armstrong and B.L. Colborn, Note on Calculated Results for Particle Spectra Produced in Thin Pb and U Targets and Comparison with Experimental Data, Report No AA-TN-814908 (unpublished)

[5] D. Filges, Calculated Neutron and Charged Particle Spectra in Thin Pb and U-Targets and Comparison with Experimental Data, private communication, 1982

[6] S.D. Howe, S. Cierjacks, Y. Hino, F. Raupp, M.T. Rainbow, M.T. Swinhoe and L. Buth, Differential Production Cross Sections for Charged Particles Produced by 590 MeV Proton Bombardment of Thin Metal Targets, ICANS-V, Proc. 5th Meeting of the Int. Coll. on Advanced Neutron Sources, G.S. Bauer and D. Filges (Eds.), Jül-Conf-45, p. 313-331, 1981

[7] R.A. Cecil, B.D. Anderson and R. Mady, Improved Predictions of the Neutron Detection Efficiency for Hydrocarbon Scintillators from 1 to about 300 MeV, Nucl. Instrum. Meth. 161, 439 (1979)

[8] S. Cierjacks, M.T. Swinhoe, L. Buth, S.D. Howe, F. Raupp, H. Schmitt and L. Lehmann, Nucl. Instrum. Meth. 192, 407 (1982)

[9] Y. Hino, S. Cierjacks, S.D. Howe, M.T. Rainbow, M.T. Swinhoe and L. Buth, Measurement of the High Energy Component of the Neutron Spectrum from a Moderated Source, ICANS-V, Proc. 5th Meeting of the Int. Coll. on Advanced Neutron Sources, G.S. Bauer and D. Filges (Eds.), Jül-Conf-45, p. 489-495, 1981

[10] W.R. Burrus, Utilization of a priori Information by Means of Mathematical Programming in the Statistical Interpretation of Measured Distributions, ORNL-3743, Oak Ridge National Laboratory, 1965

KERNFORSCHUNGSZENTRUM KARLSRUHE
INSTITUT FÜR NEUTRONENPHYSIK UND REAKTORTECHNIK

1. Nuclear Data Evaluation

1.1 Level Densities for Actinides Corrected for Unresolved Multiplets

F.H. Fröhner

For statistical-model calculations of resonance-averaged partial cross sections one needs average partial widths and, in particular, level densities. The latter are most directly obtained in the resolved resonance region by counting observed peaks and correcting for missing levels. In a recent benchmark exercise [1] it turned out that available missing-level estimation methods (with the exception of those based on Monte Carlo generation of mock cross sections) are deficient as they do not account for levels missing in unresolved multiplets that were counted as singlets. An analytical method was newly developed to account for this resolution effect in the analysis of s-wave resonances. If one assumes that the areas of unresolved multiplet peaks are equal to the sum of the component areas it can be shown [2] that the apparent neutron widths of s-wave resonances are distributed according to

$$p(G)dG = (1-q)\ (1+v)\ \frac{e^{-x}}{\sqrt{\pi x}}\,dx \quad , \qquad x \equiv \frac{G}{2\langle g\Gamma_n^0\rangle} \quad , \tag{1}$$

with

$$v = \sqrt{\pi}z\ e^{z^2}\ (1 + \mathrm{erf}\ z) \quad , \qquad z \equiv q\sqrt{x} \quad . \tag{2}$$

where G is the apparent reduced neutron width times the spin factor g, Γ_n^0 is the reduced neutron width, <...> denotes the ensemble average and q is the fraction of level spacings smaller than the minimum resolvable level separation. One can now base the estimation of missing levels on this distorted Porter-Thomas distribution instead the undistorted one and thus include resolution effects without need for Monte Carlo calculations [2]. The statistical resonance analysis code STARA [3] which estimates s-wave strength functions and mean level spacings from given samples of resonance energies and neutron widths was modified accordingly. The following table shows STARA results for U and Pu isotopes with

and without correction for unresolved multiplets. For the well studied nuclides ^{235}U and ^{238}U the corrections are quite small (1-2%). For the Pu isotopes they are about 5% and for ^{241}Pu even 20%, which indicates lower quality of the resonance data with significant numbers of unresolved multiplets. The corrections cause a corresponding relative change of almost equal magnitude in the average capture, fission and inelastic-scattering cross sections calculated with the level-statistical model.

Table I - Results of statistical resonance analysis without and with account of levels lost in unresolved multiplets

Target Nucleus	Energies (eV)	Sample Size	S_0 (10^{-4})	D_0 (eV)	Multiplets Considered?	Resonance Parameter Source
^{235}U	0-100	196	.97±.12	.44±.01	no	Moore+ 78
			.96±.12	.43±.01	yes	
^{238}U	0-4000	188	1.16±.13	20.4±.2	no	Keyworth+ 78
			1.15±.12	20.3±.2	yes	
^{239}Pu	0-660	257	1.26±.12	2.28±.05	no	Derrien 74
			1.27±.12	2.20±.05	yes	
^{240}Pu	0-3000	172	1.03±.10	13.1±.5	no	KEDAK-3 77
			1.02±.10	12.4±.7	yes	
^{241}Pu	0-161	123	1.20±.18	.90±.04	no	KEDAK-3 77
			1.23±.13	.73±.08	yes	
^{242}Pu	0-500	37	.82±.26	12.6±.6	no	KEDAK-3 77
			.83±.27	13.3±.4	yes	

References

[1] P. Ribon, NEANDC(E) 213-AL, 1st part (1980);
P. Ribon and P. Johnston, NEANDC(E) 213-AL, 2nd part (1981)

[2] F.H. Fröhner, Proc. Meeting on Uranium and Plutonium Isotope Resonance Parameters, INDC(NDS)-129/GJ, IAEA Vienna (1981)

[3] F.H. Fröhner, Proc. Spec. Meeting on Neutron Cross Sections of Fission Product Nuclei, RIT/FIS-LDN(80)1, Bologna (1979), p. 145

1.2 Neutron Cross Sections for Actinides

B. Goel, F. H. Fröhner, H. Jahn

The evaluation for the isotopes ^{241}Am, ^{242m}Am, ^{243}Am and ^{244}Cm has been completed. These actinides are marked with the lack of experimental data, though during the course of evaluation some data became available, so that for ^{241}Am enough data is now available to check the models used for their reliability. In the resonance region the data were analysed by the R matrix theory and in the MeV region the optical model was used. The quality of experimental data did not warrant a sophistication of the calculation. The spherical optical model was considered to be adequate. The potential parameters were established by a thorough study of the neighboring nucleus ^{238}U. The so obtained Wood-Saxon potential has the parameters:

$$V = 47.01 \text{ MeV} - 0.267\ E - 0.00118 \text{ MeV}^{-1}\ E^2 ,$$

$$W = 9.0 \text{ MeV} - 0.53\ E ,$$

$$R_r = 1.21 \text{ fm } A^{1/3} , \qquad R_i = 1.298 \text{ fm } A^{1/3} ,$$

$$a_r = 0.66 \text{ fm} , \qquad a_i = 0.48 \text{ fm} .$$

Fig. 1 shows the total cross section calculated with this potential together with measured data. It should be noted that the experimental data by Phillips and Howe became available only after the potential had been finalised.

Fig. 2 shows the $^{242}Am(n,\gamma)$ cross section in the energy range from 1 keV to 10 MeV. In the region of overlap the two evaluation methods show good agreement. The situation for other isotopes is similar.

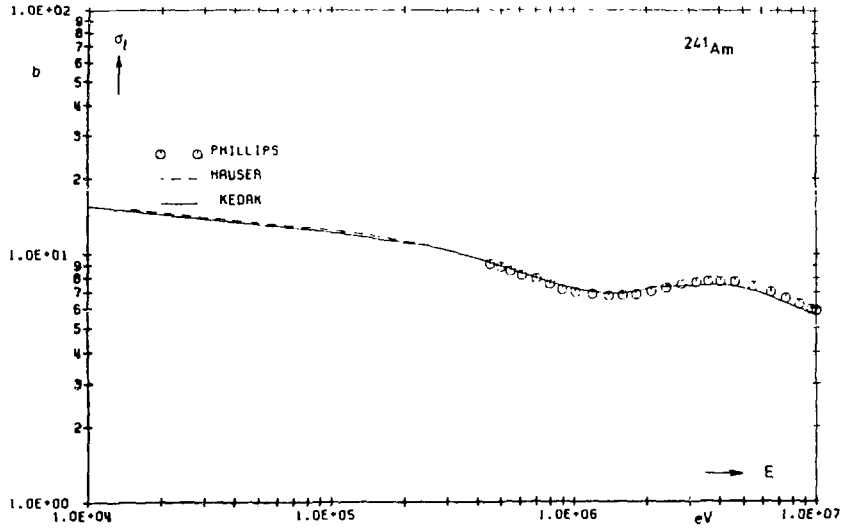

Fig. 1 - Predicted and measured total cross sections for ^{241}Am+n. Above 200 keV the global HAUSER calculation was adopted for KEDAK, below it was replaced by a FITACS fit which includes information from resolved resonances and from unresolved fission and capture data.

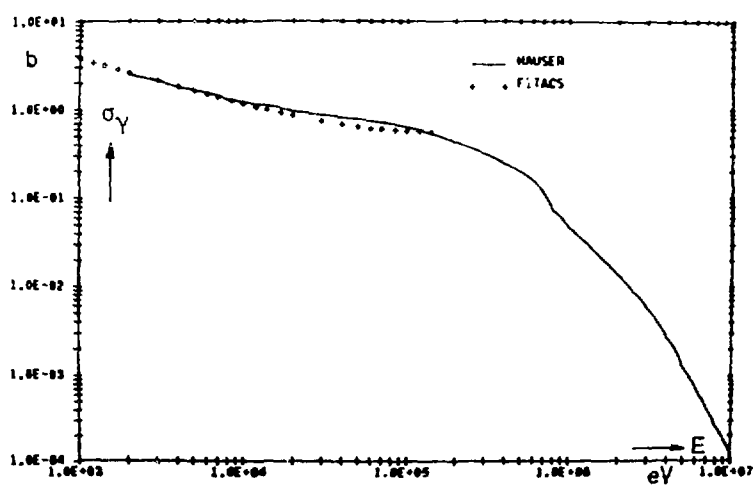

Fig. 2 - Calculated capture cross sections for ^{242m}Am+n. HAUSER curve represents global prediction, FITACS points represent extrapolation from resolved resonance region which is also consistent with fission cross section data up to 100 keV.

1.3 Resonance Integrals for Am and Cm Isotopes

B. Goel

During the course evaluation (1.2) a wide range in the published values for the resonance integrals was observed. Due to the presence of strong resonances near the Cd-cutoff energy, the measured values of the resonance integral for the actinide isotopes are very sensitive to the effective cutoff energy. The resonance integrals for ^{241}Am, for example, change by a factor of about 2.5 by changing the Cd-cutoff energy from 0.3 eV to 0.6 eV (Fig. 1). For ^{241}Am all but one of the integral measurements can be reconciled with the evaluation if cutoff energy is properly accounted for. For other isotopes there are some discrepancies that need further explanation.

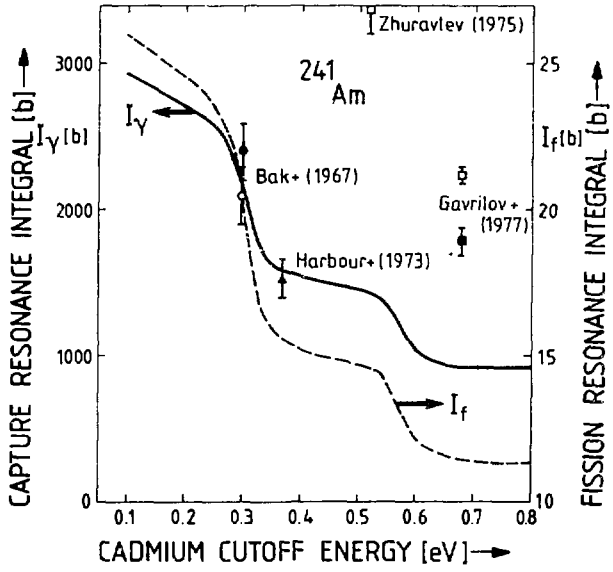

Fig. 1
RESONANCE INTEGRALS FOR ^{241}Am AS A FUNCTION OF Cd-CUTOFF ENERGY

2. Data for Fusion Reactor

2.1 DT Fusion Reaction Cross Section

B. Goel

In the calculation of reaction rates for DT fusion energy dependence of the fusion cross section is generally described by the Gamow's barrier penetration formula. This leads to a rather simple formula for the Maxwellian reactivities:

$$\langle \sigma v \rangle = \left(\frac{a}{kT}\right)^{2/3} \exp\left\{\left(\frac{b}{kT}\right)^{1/3}\right\}$$

The reactivity values calculated with this formula, as shown in Fig. 1, differ considerably from the exact calculation. The DT cross section was evaluated up to 10 MeV (Fig. 2) and Maxwellian reactivities were calculated using the evaluated data.

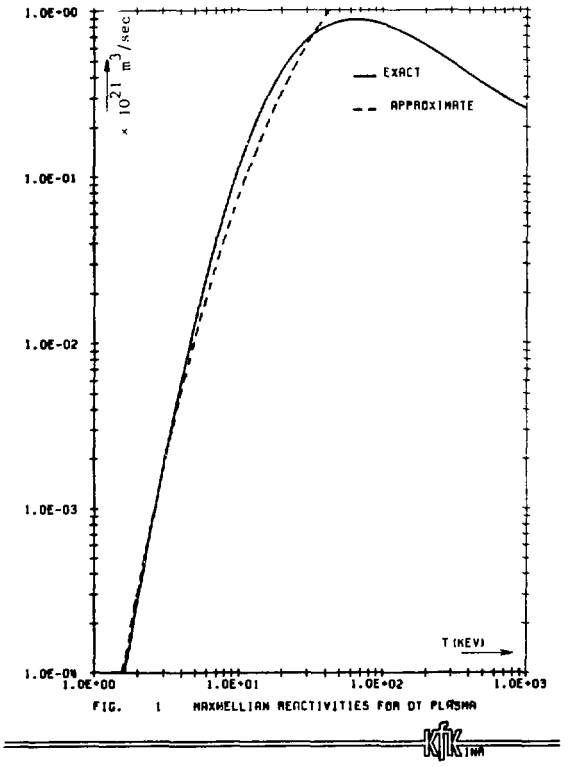

FIG. 1 MAXWELLIAN REACTIVITIES FOR DT PLASMA

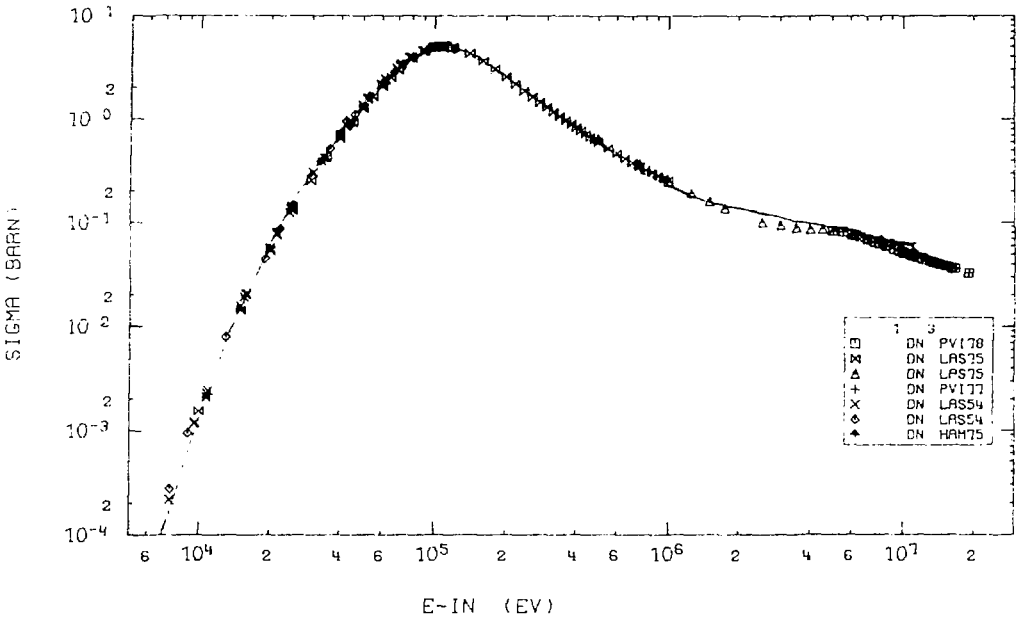

Fig. 2: Comparison of Experimental Data with the Calculated Cross Section for T(d,n)α Process

INSTITUT FÜR CHEMIE (1): NUKLEARCHEMIE
KERNFORSCHUNGSANLAGE JÜLICH

1. Neutron Data

1.1 Study of (n,t) and (n,^{3}He) Reactions

S.M. Qaim, R. Wölfle

In continuation of our radiochemical studies on fast-neutron induced trinucleon emission reactions, the (n,t) reactions were investigated by vacuum extraction and gas phase "low-level" β^- counting of tritium. Cross sections were measured for the target elements Ti, V, Mn, Fe, Cu, Mo, Ag, Ta, Tl, Pb and Bi irradiated with 30 MeV d(Be)-break up neutrons. A constant cross-section value of 0.55 $\pm$ 0.15 mb over the whole mass region suggests that possibly surface reactions are involved.

A measurement of the excitation function of the (n,t) reaction on ^{59}Co in the energy region of 15 to 20 MeV was completed in collaboration with the CBNM Geel (H. Liskien). Detailed Hauser-Feshbach calculations on the (n,t) reactions on ^{27}Al, ^{59}Co and ^{93}Nb revealed [1] that the statistical contributions decrease with the increasing mass of the target nucleus. A summary of the results is given in Fig. 1.

The (n,^{3}He) reactions were investigated radiochemically and cross sections were measured for the target nuclides ^{133}Cs, ^{146}Nd, ^{165}Ho, ^{174}Yb, ^{186}W and ^{197}Au irradiated with 53 MeV d(Be) break-up neutrons. Mass spectrometric studies on the relative ^{3}He/^{4}He emission were extended to target elements with A > 120.

1.2 Cross Section Measurements of Hydrogen and Helium Producing Reactions induced by 4 to 9 MeV Neutrons

S.M. Qaim, R. Wölfle

(Relevant to request identification numbers: 752244F, 762107F, 762108F, 76224F, 792209R)

Our radiochemical studies on hydrogen and helium generating reactions at 14 MeV (cf. [2 and 3]) and with break-up neutron spectra have now been extended to the energy region of 4 to 9 MeV. For this purpose a dd-gas target has been constructed at our variable energy compact cyclotron CV 28. The

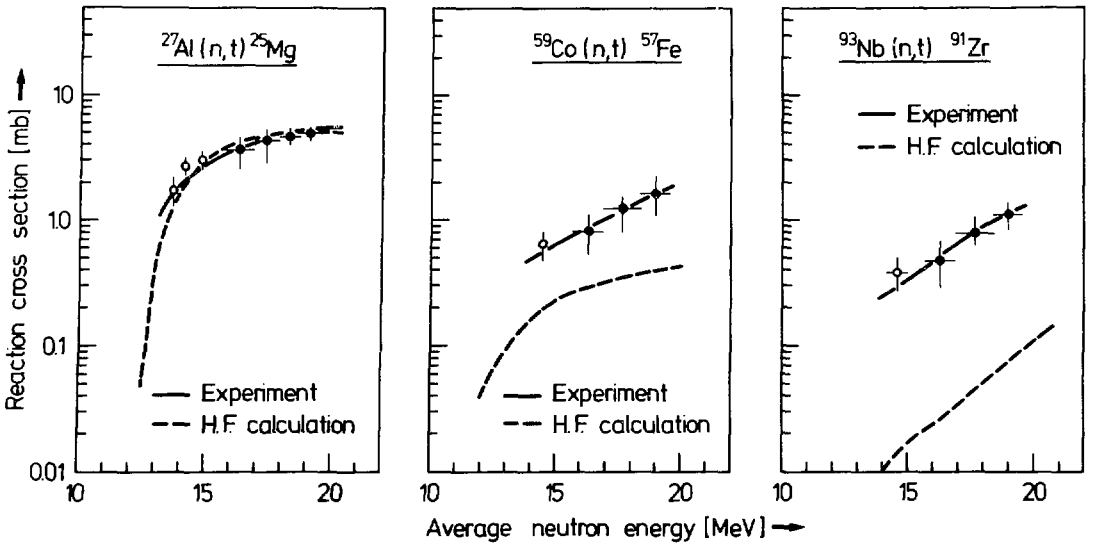

Fig. 1 Excitation functions of (n,t) reactions on ^{27}Al, ^{59}Co and ^{93}Nb. Points and solid lines describe the experimental data and trends; the dashed lines give results of Hauser-Feshbach calculations [1].

deuteron beam passes through a thin Havar foil and enters a 3.7 cm x 2,0 cm dia. cell filled with D_2 at 1.8 bar. A 100 µm Mo-foil is used as beam-stop which is cooled by a jet of air. Generally deuteron beams of 5 µA are used. The samples to be irradiated with quasi-monoenergetic neutrons are placed at 0° to the incident beam. The shape of the neutron spectrum has been checked qualitatively using an NE 213 scintillator and the neutron flux densities are determined using known monitor reactions.

The excitation function for the reaction ^{58}Ni(n,α)^{55}Fe ($T_{1/2}$ = 2,7 y) has been measured for the first time. About 10 g Ni was irradiated at each energy. Due to its soft radiation (5.8 keV X-rays) ^{55}Fe cannot be determined easily. By means of a radiochemical separation of iron and electrolytic preparation of a thin source, followed by X-ray spectroscopy using a Si(Li) detector, it was possible to determine the cross sections.

1.3 Measurement of Excitation Function of $^{7}Li(n,n't)^{4}He$ Reaction

H. Liskien*, S.M. Qaim, R. Wölfle

(Relevant to request identification numbers: 724007F, 724008F, 732004F, 762246F, 781159F, 792105F)

Cross sections have been measured using separation and gas phase counting of tritium over the energy range of threshold to 8 MeV. The total errors in the data amount to about 5 %. The excitation function is about 15 % lower than the ENDF B IV curve. Measurements in the energy region of 13 to 16 MeV are in progress.

2. Charged Particle Data for Radioisotope Production

S.M. Qaim, G. Stöcklin, J.H. Zaidi**

In continuation of our studies [4-8] on the production of medically important short-lived radionuclides, cross section measurements were performed on the $^{122}Te(d,n)^{123}I$ reaction up to a deuteron energy of 40 MeV.

The most commonly used method for the production of ^{123}I at a relatively low-energy cyclotron is the $^{124}Te(p,2n)^{123}I$ reaction. The associated ^{124}I impurity, however, is rather high ($\sim$ 1 % at EOB). The (d,n) reaction on ^{122}Te appeared to be promising. Since the excitation functions for this and the competing reactions were not known, we determined them experimentally using the stacked-foil technique. For this purpose thin samples of ^{122}Te (96.45 % enriched) were obtained by electrodeposition on Ti-foils. The results are shown in Fig. 2.

In addition to the (d,xn)-reactions, excitation functions for the $^{122}Te(d,p)^{123}Te$, $^{122}Te(d,p2n)^{121m+g}Te$ and $^{122}Te(d,\alpha)^{120}Sb$ reactions were also measured. A comparison of the data shows that in this mass region the excited nucleus emits neutrons more favourably than the charged particles.

---

* CBNM, Geel, Belgium

** On leave from Pakistan Institute of Nuclear Science and Technology, Rawalpindi, Pakistan

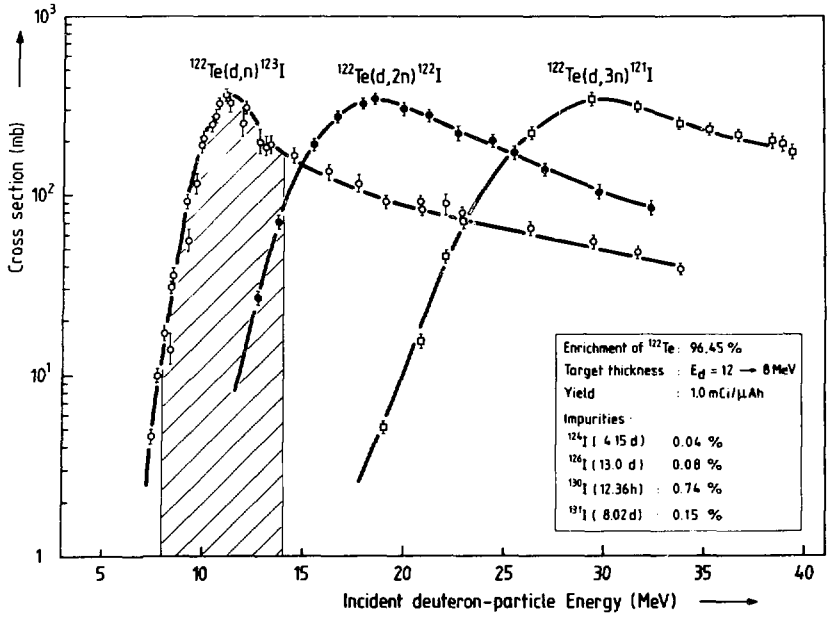

Fig. 2 Excitation functions for (d,xn) reactions on enriched ^{122}Te. The optimum energy range for the production of ^{123}I via the (d,n) reaction at a compact cyclotron is E_d = 14 → 8 MeV.

For a target thickness corresponding to E_d = 12 → 8 MeV the levels of impurities ^{124}I, ^{125}I, ^{126}I and ^{131}I were found to be negligibly small, the major impurity being 12.4 h ^{130}I (0.74 % at EOB). The (d,n) method, however, appears to be only of limited application since the thick target yields are rather low.

In addition to the experimental work on excitation functions, a detailed survey of nuclear data relevant to the production of short-lived radioisotopes was carried out [9].

References

[1] S.M. Qaim, R. Wölfle, H. Liskien, Excitation functions of (n,t) reactions on ^{27}Al, ^{59}Co and ^{93}Nb, Phys. Rev. C25 (1982) 203

[2] S.M. Qaim, 14 MeV neutron activation cross sections, Handbook of Spectroscopy, Vol. III, CRC Press, Inc., Boca Raton, Florida, USA (1981) p. 141

[3] S.M. Qaim, A systematic study of (n,d), (n,n'p) and (n,pn) reactions at 14.7 MeV, Nucl. Phys. A382 (1982) 255

[4] S.M. Qaim, R. Weinreich, Production of ^{75}Br via the ^{75}Kr precursor: Excitation function for the deuteron induced nuclear reaction on bromine, Int. J. appl. Radiat. Isotopes 32 (1981) 823

[5] He Youfeng, S.M. Qaim, G. Stöcklin, Excitation functions for ^{3}He-particle induced nuclear reactions on ^{76}Se, ^{77}Se and ^{nat}Se: Possibilities of production of ^{77}Kr, Int. J. appl. Radiat. Isotopes 33 (1982) 13

[6] H. Backhausen, G. Stöcklin, R. Weinreich, Formation of ^{18}F via its ^{18}Ne-precursor: Excitation functions of the reactions ^{20}Ne(d,x)^{18}Ne and ^{20}Ne(^{3}He,αn)^{18}Ne, Radiochim. Acta 29 (1981) 1

[7] Z.B. Alfassi, R. Weinreich, The production of positron emitters ^{75}Br and ^{76}Br: Excitation functions and yields for ^{3}He- and α-particle induced nuclear reactions on arsenic, Radiochim. Acta, in press

[8] S.M. Qaim, H. Ollig, G. Blessing, A comparative investigation of nuclear reactions leading to the formation of short-lived ^{30}P and optimization of its production via the ^{27}Al(α,n)^{30}P process at a compact cyclotron, Int. J. appl. Radiat. Isotopes, in press

[9] S.M. Qaim, Nuclear data relevant to cyclotron produced short-lived medical radioisotopes, Radiochim. Acta, in press

INSTITUT FÜR REINE UND ANGEWANDTE KERNPHYSIK
UNIVERSITÄT KIEL, FORSCHUNGSREAKTOR GEESTHACHT

Fast-Chopper Time-of-Flight Spectrometer

H.-G. Priesmeyer, P. Fischer, U. Harz, B. Soldner

1. Total Cross Section of Bound Proton in Zirconiumhydride at 77 K

The Fast-Chopper has been equipped with a cryo-samplechanger suitable to cool material down to 4 K. The first measurements on $ZrH_{1,92}$ in the energy range 0.05 eV to 1.2 eV have been made at 77 K. Figure 1 shows the result: the first minimum corresponding to an energy level of the proton harmonic oscillator in Zirconium is a sharp cusp as predicted by Fermi's theory. Structures which have been seen in a previous experiment do not seem to be realistic. Neutron upscattering in the minima and the transition of the cross-section to the free-proton value at higher energies can be observed.

The sample is positioned in the neutron beam by means of a magnetic clutch and the positions "in beam" and "open beam" are indicated using electrooptical reflectors: both clutch and position signals operate well even at 4 K.

2. Comparative Measurements between a Li-6 Glass and a He-3 High Pressure Gas Scintillator

A He-3 high-pressure gas scintillation neutron detector has been compared to a Li-6 glass scintillator type NE 912. While the Li-6 pulse height spectra of our integral-line assemblies show an energy resolution of about 18 %, the corresponding figure for the He-3 scintillator is in the vicinity of 7o %. n,γ-discrimination properties by pulse height were investigated using Cf-252 neutrons and Co-60 γ-rays. Time-of-flight spectra were taken in order to determine the actual signal-to-background ratios with either detector at the 5 m station of the Kiel Fast-Chopper spectrometer. Under these conditions the He-3 detector shows an advantage over the glass scintillator. Efficiencies of the two detectors were compared in the 2 keV and 24 keV filtered beam neutron fields of the PTB reactor, Braunschweig. The detection efficiency of the glass is about three times as high as that of the high pressure detector.

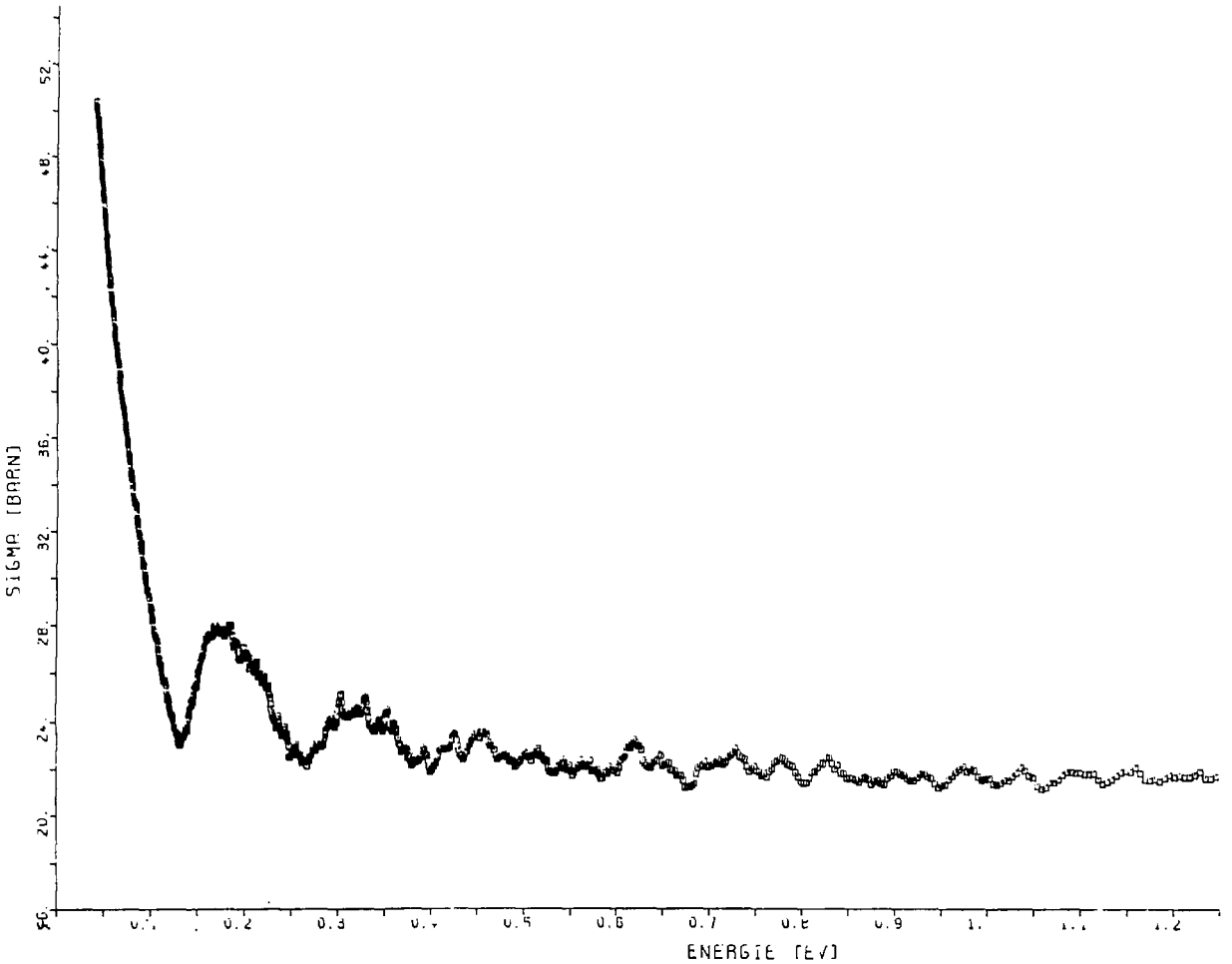

Figure 1: Total cross section of the proton bound in Zirconium at 77 K (preliminary results)

3. Resonance Transmissions of Highly Radioactive Material

Resonance transmissions of two recent chopper runs are given in Figures 2 (resolution 49.7 ns/m) and 3 (resolution 15.8 ns/m). Both samples have activities in the order of 600 Curies. The fissionproduct-cesium measurements are to be compared to earlier results. The time interval elapsed between the two experiments allowed for about 10 % of the ^{137}Cs to decay. This gives a chance to isotopically identify the resonances. The results of the analysis of these data will be published in Kerntechnik/ATOMKERNENERGIE.

4. Concept of a Li-D-Thermal-to-Fast Neutron Converter

The old idea to initiate the D-T reaction by a Li-6-D converter in a thermal reactor spectrum has recently been put forward again. It was recommended to investigate the feasability of such a converter in fusion reactor materials work [BNL-NCS-41245, Vol.I, p.17].

Careful design of the converter (high D-loading and consideration of the energy-dependence of the D-T reaction cross-section) could possibly increase the neutron yield. Such an effort is necessary since the conversion factor of 10^{-4} is comparable to the fast neutron fraction (E_n > 12 MeV) of the fission neutron spectrum in a reactor, as can be calculated from the WATT formula.

A fast neutron converter would have several advantages:

- it can extend existing irradiation capabilities of a light-water reactor to an energy range of growing interest (possibly at low cost)
- it may be build large enough for material irradiation purposes
- it can be used for fast-neutron radiography, for dosimetry development, for spectrum-averaged cross-section measurements (e.g. gas-production cross-sections), or activation analysis.

Preliminary calculations on an optimum design of the converter were begun and it shall be tried to varify the previous experimental results first. For an experimental investigation one of the tangential beam holes at FRG-1 shall be used where a CO_2-driven rabbit-system has been installed.

Figure 2: Transmission of Cs 133/135/137 Chloride from 30 eV to 1200 eV

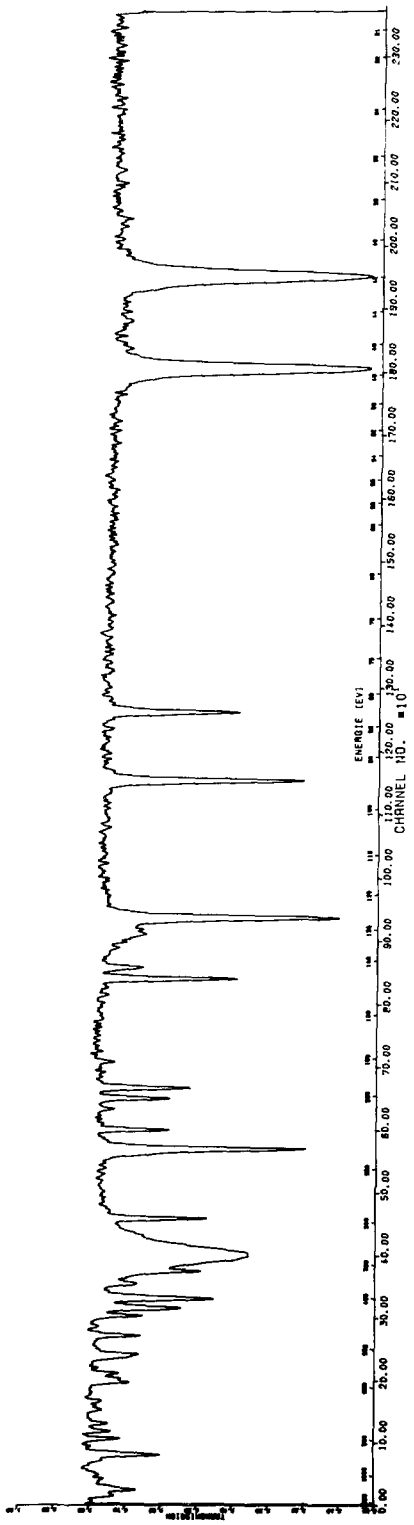

Figure 3: Transmission of gross fissionproduct mixture from 3 eV to 60 eV

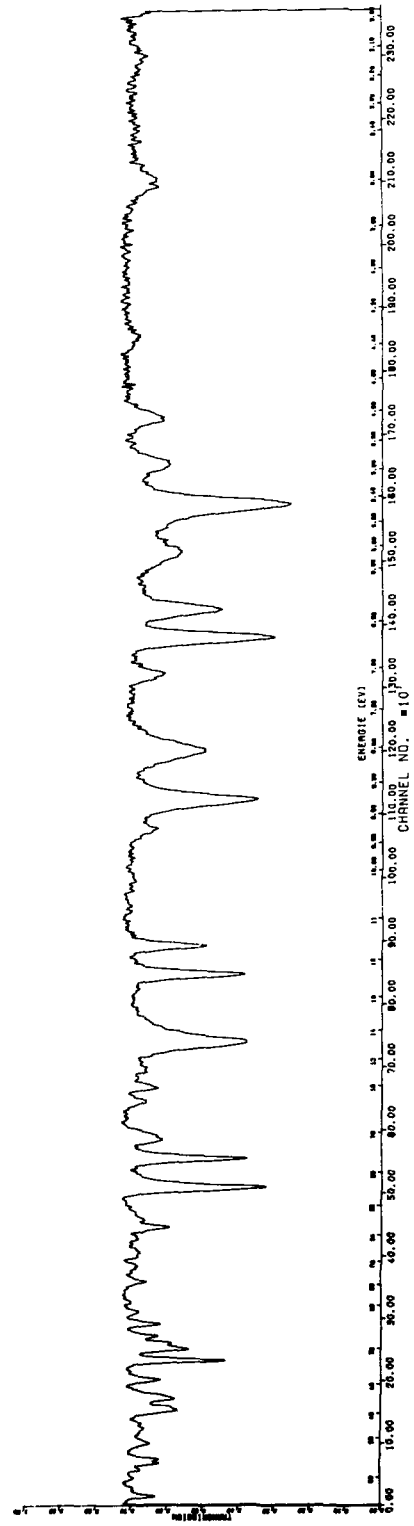

5. Publications

P. Fischer, U. Harz, H.-G. Priesmeyer: Energieeichung des IKK-Fast Choppers mit U-238 Standards. Die Resonanzparameter des Iridiums im Energiebereich bis 1.5 eV. GKSS 81/E/17.

P. Fischer, U. Harz, H.-G. Priesmeyer: Die Neutronentransmission von Spaltproduktcäsium im Resonanzbereich. DPG-Verhandlungen 1981, S. 677.

P. Fischer, U. Harz, H.-G. Priesmeyer: Neutron Resonance Parameters of 99-Tc in the Energy Range Between 4.5 eV and 25 eV. ATKE 38 (1981), 63.

H.-G. Priesmeyer, P. Fischer, U. Harz: Neutron Physics Activities At The FRG-1 Research Reactor. IAEA-SR-77/67.

INSTITUT FÜR KERNCHEMIE
UNIVERSITÄT ZU KÖLN

1. Integral Excitation Functions of Charged Particle Induced Reactions for Energies up to 45 MeV/A

R.Michel, G.Brinkmann, M.Galas and R.Stück

1.1. α-Induced Reactions on Titanium, Vanadium and Mangenese

Completing a systematic investigation of α-induced reactions on target elements $22 \leq Z \leq 28$ fifty excitation functions were measured for the production of radionuclides $42 \leq A \leq 58$ from natural titanium,vanadium and manganese for 15 MeV $\leq E_\alpha \leq$ 172.5 MeV.

Because of the rather high (up to ~ 5 %) abundance of titanium in the lunar surface, this element deserves particular interest as target element with regard to certain cosmochemical applications. So the new measurements on titanium [1] - together with earlier ones on Fe and Ni [1] - now permit a quantitative description of the interaction of solar α-particles with extraterrestrial matter. Analogous model calculations were already performed for the interaction of solar protons with the lunar surface [2] as well as with meteorites and cosmic dust [3].

Moreover, these experimental excitation functions are useful for testing actual theories of nuclear reactions. So the experimental data were compared with theoretical predictions on the basis of the hybrid model of preequilibrium reactions [4]. The faculty of this model for "a priori" calculations is of high value in the field of applications of cross sections.

There are discrepancies, however, between the newly measured excitation functions and the theoretical ones which are similar to those described earlier [5] for cobalt. These deviations give evidence for a greater complexity of the initial reaction phase of α-induced reactions than accounted for by the hybrid model in the form of "OVERLAID ALICE" [6]. In particular, incomplete break-up of the incoming α-particle will result in a lower excitation energy of the compound system, thus rising the cross sections for exit channels with small differences in target and product nuclide. An example of this type is given in Fig.1. At 170 MeV the experimental data for $Ti(\alpha,3pxn)^{48}Sc$ are underestimated by theory by more than a factor of 10. But since Ti has 5 stable isotopes here it is difficult

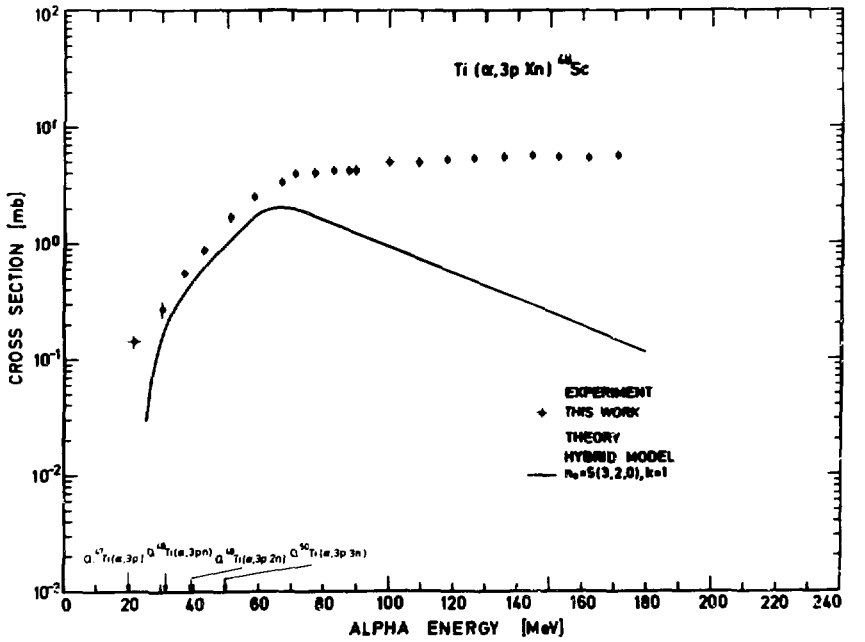

Fig.1: Experimental cross sections and hybrid model calculations for Ti(α,3pxn)^{48}Sc.

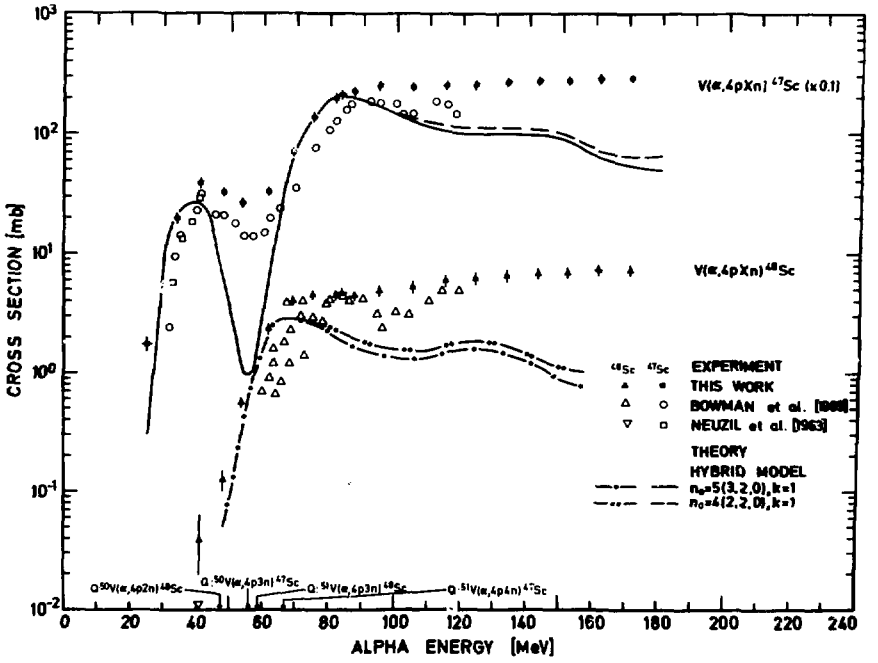

Fig.2: Experimental and theoretical excitation functions for the production of ^{47}Sc and ^{48}Sc from vanadium. For the work of other authors see references [8,9].

to attribute the discrepancies to a particular reaction channel.

In the case of V and Mn [7] which are - or at least can be regarded as - single isotope targets, the experimental cross sections permit a more detailed theoretical analysis. Exemplarily in Fig.2 a comparison of experimental and hybrid model data for V(α,4pxn)-reactions leading to ^{47}Sc and ^{48}Sc is made. For ^{47}Sc in the energy region between 50 and 60 MeV pre-equilibrium α-emission in the reaction ^{51}V(α,2α)^{47}Sc is to be observed which is not described by theory. At higher energies, the evaporation peak of the ^{51}V(α,2p2n)^{47}Sc-reaction is adequately reproduced. Above 100 MeV, however, the experimental cross sections show a strong levelling-off which is not to be seen in the calculations. Also for the ^{51}V(α,4p3n)^{48}Sc-reaction, the calculated cross sections at 170 MeV deviate from the experimental ones by an order of magnitude. Here, possible break-up effects may be important, so that the actual reaction is to be attributed rather to ^{51}V(n,α)^{48}Sc than ^{51}V(α,4p3n)^{48}Sc. A more detailed analysis of the excitation functions measured is in progress.

1.2. Cross Sections for the α-Induced Production of ^{62}Zn, ^{61}Cu and ^{57}Ni from Nat. Nickel

For the investigation of α-induced reactions on Mn target foils were used which were made of a Mn/Ni alloy (Goodfellow Metals, Ltd., U.K.) consisting of 88 % Mn and 12 % Ni. All the nuclides produced by α-induced reactions on Mn had to be corrected for a contribution from Ni. For this purpose our earlier data on Ni [1] were used and this correction resulted only in a very small increase of the errors of the individual cross sections. In spite of the dominating Mn content of the foils it was possible to determine 3 excitation functions for the production of ^{62}Zn, ^{61}Cu and ^{57}Ni from nat. Ni. In Table 1 the nuclear data used for the evaluation of the cross sections are given, together with a survey on the nuclear reactions contributing to the production of these nuclides and the respective Q-values. All the cross sections determined (Table 2) are in very good agreement with our earlier measurements [1,13].

1.3. Production of ^{24}Na and ^{22}Na by ^{2}H-Induced Reactions on Aluminium

Extending our earlier studies on p- and α-induced reactions on target elements $22 \leq Z \leq 28$ to ^{2}H- and ^{3}He-induced reactions, we investigated such reactions on Al up to 45 MeV/A in order to allow for a better control of the beam monitoring procedure [e.g.5] during the experiments in preparation.

Nuclide	Halflife	E_γ[KeV]	I_γ[%]	Q-Values [MeV]	
^{62}Zn	9.13 h	548.35	15.34	^{58}Ni(α,γ):+ 3.3	^{60}Ni(α, 2n):-17.1
		596.56	26.00	^{61}Ni(α, 3n):-24.9	^{62}Ni(α, 4n):-35.5
				^{64}Ni(α, 6n):-52.0	
^{61}Cu	3.3 h	283.0	12.8	^{58}Ni(α, p):- 3.1	^{60}Ni(α, p2n):-23.5
				^{61}Ni(α, p3n):-31.3	^{62}Ni(α, p4n):-41.9
				^{64}Ni(α, p6n):-58.4	
^{57}Ni	36 h	1377.62	84.9	^{58}Ni(α,2p3n):-40.5	^{60}Ni(α,2p5n):-60.9
		1919.57	14.97	^{61}Ni(α,2p6n):-68.7	^{62}Ni(α,2p7n):-79.3
				^{64}Ni(α,2p9n):-95.8	

Table 1: Halflives [10], γ-energies and branching ratios [11] used for the determination and Q-values of the contributing reactions [12].

E_α [MeV]	^{62}Zn	^{61}Cu	^{57}Ni	E_α [MeV]	^{62}Zn	^{61}Cu	^{57}Ni
171.15 ± 0.36		5.93 ± 0.53	35.8 ± 3.6	88.4 ± 1.1	1.17 ± 0.48	27.0 ± 3.2	37.9 ± 4.2
162.24 ± 0.53		6.23 ± 0.56	38.5 ± 4.2	78.68 ± 0.68	2.5 ± 1.4	34.0 + 4.4	38.5 ± 3.1
152.88 ± 0.64		7.7 ± 1.0	38.4 ± 3.8	67.53 ± 0.79	4.4 ± 1.8	42.8 ± 5.1	28.0 ± 2.8
144.37 ± 0.72		8.6 ± 1.1	40.9 ± 3.7	57.77 ± 0.90	3.7 ± 1.5	63.7 ± 5.7	19.1 ± 2.1
135.32 + 0.79		9.6 ± 1.3	37.7 ± 3.4	49.4 ± 1.0	5.8 ± 1.4	111. ±11.	18.0 ± 2.2
125.91 ± 0.83		10.9 ± 1.5	38.4 ± 3.5	39.8 ± 1.1	16.4 + 2.3	86.2 ± 9.5	25.7 ± 2.3
117.40 ± 0.92	0.73 ± 0.43	13.9 ± 1.8	37.5 ± 4.1	32.8 ± 1.3	34.0 ± 5.4	43.9 ± 5.3	27.3 ± 2.7
108.43 ± 0.98		18.5 ± 2.2	39.4 ± 3.9	24.4 ± 1.5	13.2 ± 2.0	160. ±19.	6.07 ± 0.69
98.8 ± 1.0		19.6 + 2.4	35.8 ± 3.6	12.7 ± 2.1	2.85 + 0.66	358. ±47.	
88.70 ± 0.50	1.76 ± 0.97	24.6 ± 2.7	37.9 ± 4.2				

Table 2: Cross sections [mb] for the production of ^{62}Zn, ^{61}Cu and ^{57}Ni from natural nickel.

E_d[MeV]	^{24}Na	^{22}Na	E_d[MeV]	^{24}Na	^{22}Na
84.09 ± 0.48	22.2 ± 1.8	36.2 ± 2.3	46.82 ± 0.71	24.2 ± 1.3	26.1 ± 1.6
78.51 ± 0.62	22.1 ± 1.5	35.7 ± 2.2	42.6 ± 1.1	27.1 ± 1.8	15.2 ± 0.9
77.64 ± 0.64	22.1 ± 1.5		42.34 ± 0.81	27.8 ± 1.9	17.2 ± 1.1
73.04 ± 0.72	22.1 ± 1.5	35.2 ± 2.1	41.2 ± 1.2	28.9 ± 2.0	
68.22 ± 0.79	22.0 ± 1.7	34.9 ± 2.1	38.09 ± 0.92	33.0 ± 2.0	8.04 ± 0.49
67.25 ± 0.80	22.1 ± 1.6		36.8 ± 1.2	34.2 ± 2.4	5.32 ± 0.31
62.84 ± 0.86	21.4 ± 1.5	35.5 ± 2.2	33.4 ± 1.0	41.6 ± 2.5	2.94 ± 0.19
57.37 ± 0.93	21.5 ± 1.5	35.4 ± 2.1	29.6 ± 1.1	51.1 ± 3.0	1.35 ± 0.15
52.3 ± 1.0	22.4 ± 1.8	33.2 ± 1.9	25.3 ± 1.3	61.6 ± 4.1	0.312 ± 0.027
51.1 ± 1.0	22.3 ± 1.6		21.4 ± 1.4	57.2 ± 3.7	0.0351 ± 0.0057
47.5 ± 1.1	24.0 ± 1.7	26.3 ± 1.6	16.7 ± 1.7	28.3 ± 2.0	
			12.1 ± 2.1	2.57 ± 0.22	

Table 3: Experimental cross sections mb for ^{2}H-induced reactions on aluminium.

1.4. Production of ^{24}Na and ^{22}Na by ^{3}He-Induced Reactions on Aluminium

Earlier investigations were restricted to ^{3}He-energies below 30 MeV [25,26]. Our measurements (Table 4) now extend these data up to 126 MeV. For ^{24}Na the experimental data are corrected for contributions of the ^{27}Al(n,α)^{24}Na-reaction due to secondary neutrons. However, this correction did not exceed 0.31 mbarn. In general, for both product nuclides (Figs 5 and 6) our data are in very good agreement with the earlier low energy cross sections [25,26]. The smooth shapes of the excitation functions measured demonstrates the applicability of aluminium to monitor ^{3}He-particles in the same way as it is common for p- and d-induced reactions.

In Table 3 the excitation functions for the ^{2}H-induced production of ^{22}Na and ^{24}Na from Al are given. The nuclear and decay data used for the evaluation of cross sections again were taken from ref. [10] to [12]. The experimental cross sections are corrected for a neutron background. The neutron contribution was determined below the threshold of the respective nuclear reactions.

For the reaction $^{27}Al(d,3p2n)^{24}Na$ a considerable amount of data already existed in literature (Fig.3). But only Weinreich et al. [14] and Batzel et al. [20] reported cross sections above E_d = 50 MeV. Our data are in perfect agreement with those of Weinreich et al. [14], while the data of Batzel et al. [20] show increasing deviations from the data of most of the other authors with decreasing d-energy. This is most probably due to the use of a single stack for the energy range from 190 to 10 MeV by Batzel et al. [20].

For ^{22}Na (Fig.4) only very few earlier determinations existed [17,22-24] which with one exception [24] are below 50 MeV. Our data are in agreement with those of Martens and Schweimer [17], while the data of Karpeles [22] and Ring and Litz [24] partially show considerable deviations from ours.

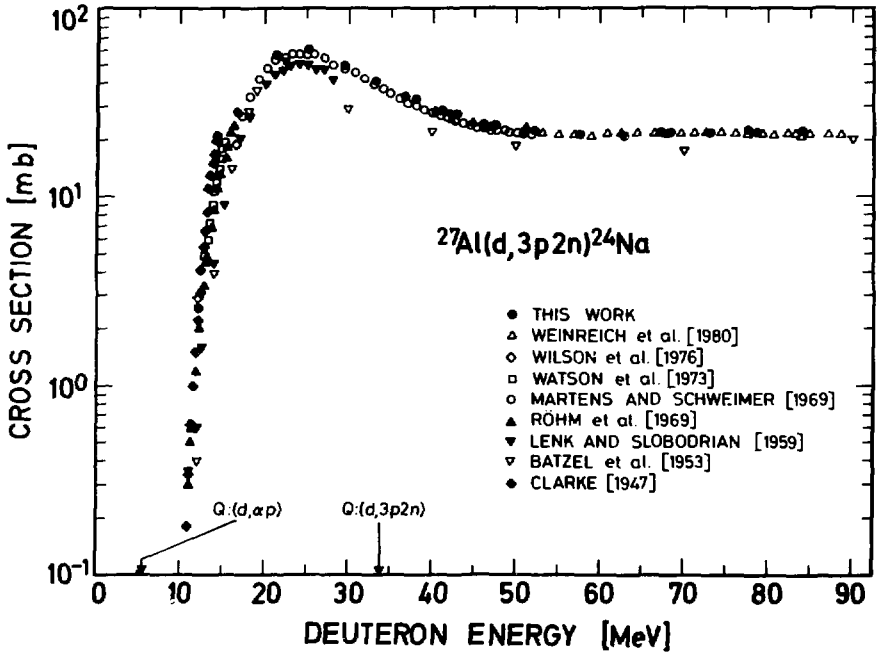

Fig.3: Excitation function for the reaction $^{27}Al(d,3p2n)^{24}Na$. For the work of other authors see references [14 to 21].

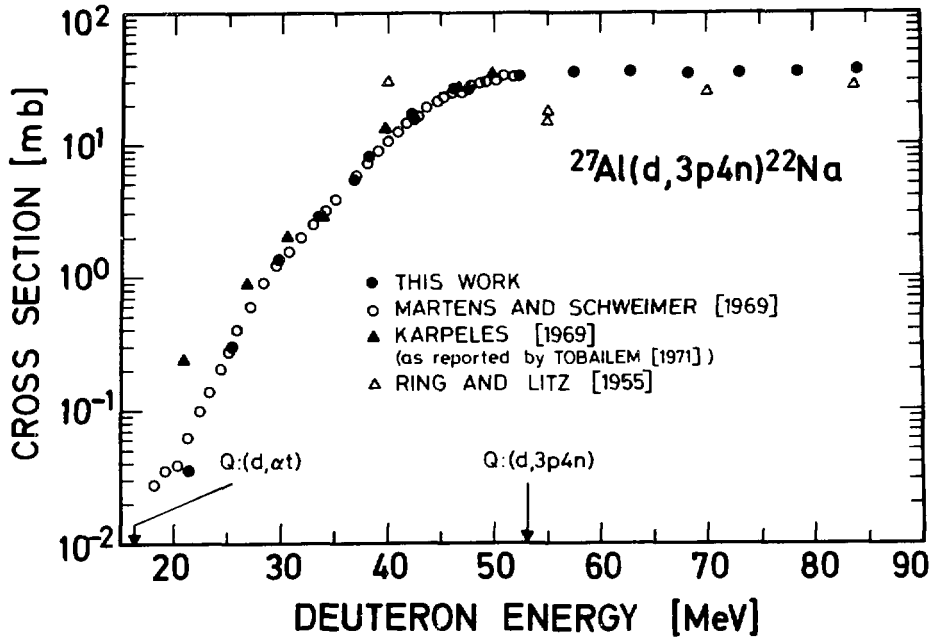

Fig.4: Excitation function for the reaction ^{27}Al(d,3p4n)^{22}Na.
For the work of other authors see references [17,22 to 24].

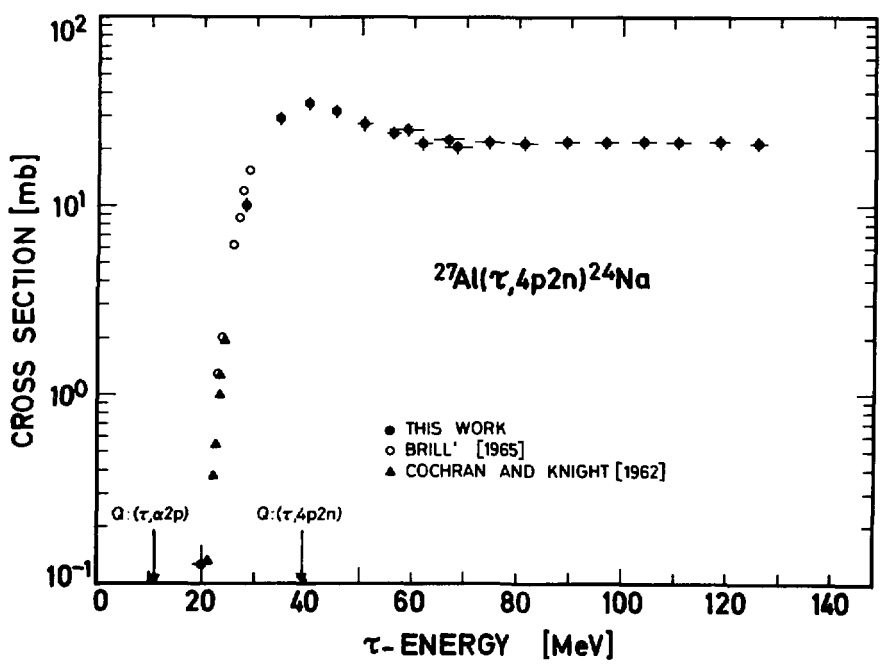

Fig.5: Excitation function for the reaction ^{27}Al(τ,4p2n)^{24}Na.
For the work of other authors see references [25,26].

E_τ [MeV]	^{24}Na	^{22}Na	E_τ [MeV]	^{24}Na	^{22}Na
125.8 ± 1.7	21.4 ± 1.4	48.3 ± 3.0	61.7 ± 1.7	21.6 ± 1.8	34.3 ± 2.5
118.4 ± 1.9	21.9 ± 1.6	49.1 ± 2.6	58.7 ± 3.4	25.4 ± 2.1	32.3 ± 1.7
110.6 ± 2.1	21.8 ± 1.6	49.6 ± 2.9	56.1 ± 1.4	24.4 ± 1.9	24.3 ± 1.7
103.9 ± 2.2	21.9 ± 1.5	50.0 ± 2.8	50.6 ± 1.5	27.4 ± 2.2	15.8 ± 1.1
96.7 ± 2.4	22.0 ± 1.5	50.9 ± 2.9	45.31 ± 0.99	31.9 ± 2.5	10.3 ± 1.0
89.3 ± 2.5	22.0 ± 1.5	51.2 ± 3.1	40.1 ± 1.1	35.0 ± 2.6	8.73 ± 0.89
81.3 ± 2.7	21.8 ± 1.7	50.2 ± 2.7	34.4 ± 1.2	28.9 ± 2.2	11.7 ± 0.8
74.4 ± 2.9	21.9 ± 1.5	49.6 ± 2.8	27.9 ± 1.2	10.1 ± 0.8	20.7 ± 1.5
68.4 ± 2.7	20.7 ± 1.5	43.1 ± 2.7	20.1 ± 1.5	0.126 ± 0.035	23.8 ± 2.4
66.9 ± 3.1	22.7 ± 1.6	43.7 ± 2.3	8.5 ± 2.4		0.281 ± 0.053

Table 4: Experimental cross sections [mb] of ^{3}He-induced reactions on aluminium.

References

[1] R.Michel, G.Brinkmann, R.Stück, J.Radioanal.Chem. (submitted)

[2] R.Michel, G.Brinkmann, J.Radioanal.Chem. 59 (1980) 467

[3] R.Michel, G.Brinkmann, R.Stück, Earth Planetary Science Letters (accepted for publication)

[4] M.Blann, Phys.Rev.Letters 27 (1971) 337

[5] R.Michel, G.Brinkmann, Nucl.Phys.A 338 (1980) 167

[6] M.Blann (1978) UR-NSRL-181

[7] R.Michel, G.Brinkmann, R.Stück (in preparation)

[8] W.W.Bowman, M.Blann, Nucl.Phys.A 131 (1969) 513

[9] E.F.Neuzil, R.H.Lindsay, Phys.Rev. 131 (1963) 1697

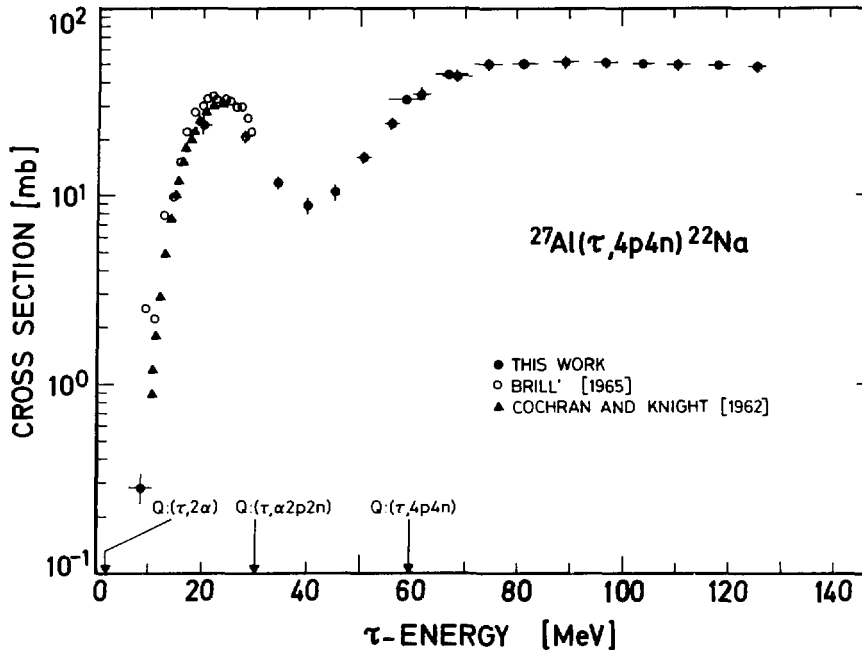

Fig.6: Excitation function for the reaction $^{27}Al(\tau,4p4n)^{22}Na$. For the work of other authors see references [25,26] .

[10] W.Seelmann-Eggebert, G.Pfennig, H.Münzel, Nuklidkarte, 4.Auflage, Gersbach-Verlag München 1974

[11] G.Erdtmann, W.Scyka (1979) Jül-Spez-34

[12] K.A.Keller, J.Lange, H.Münzel, in:Landolt-Börnstein, Numerical Data and Functional Relationships in Science and Technology, New Series, Group I, Vol.5, Part A (1973) Springer-Verlag, Berlin

[13] G.Brinkmann, Thesis University of Cologne, 1979

[14] R.Weinreich, H.J.Probst, S.M.Qaim, Int.J.Appl.Rad.Isotopes 31(1980) 223

[15] R.L.Wilson, D.J.Frantsvog, A.R.Kunselmann, C.Détraz, C.S.Zaidins, Phys.Rev.C 13 (1976) 976

[16] I.A.Watson, S.L.Waters, D.K.Bewley, D.J.Sylvester, Nucl.Instr. Meth. 106 (1973) 231

[17] U.Martens, G.W.Schweimer (1969) KFK 1083

[18] H.F.Röhm, C.J.Verwey, J.Steyn and W.L.Rautenbach, J.Inorg.Nucl. Chem. 31 (1969) 3345

[19] P.A.Lenk, R.J.Slobodrian, Phys.Rev. 116 (1959) 1229

[20] R.E.Batzel, W.W.T.Crane and G.D.O'Kelley, Phys.Rev. 91 (1953) 939

[21] E.T.Clarke, Phys.Rev. 71 (1947) 187

[22] A.Karpeles, Radiochim.Acta 12 (1969) 212

[23] J.Tobailem, C.-H.de Lassus St.Génies, L.Levecque (1971) CEA-N-1466 (1).

[24] S.O.Ring, L.M.Litz, Phys.Rev. 97 (1955) 427

[25] O.D.Brill', Soviet J.Nucl.Phys. 1 (1965) 37

[26] D.R.F.Cochran, J.D.Knight, Phys.Rev. 128 (1962) 1281

INSTITUT FÜR KERNCHEMIE

JOHANNES GUTENBERG-UNIVERSITÄT MAINZ

1. Absolute γ-ray line intensities of the Cesium- and Bariumisotopes in mass-chains 142 and 143

B. Sohnius, M. Brügger, H.O. Denschlag

The absolute γ-ray line intensities of ^{142}Cs, ^{142}Ba, ^{143}Cs and ^{143}Ba were determined using the mass separator HELIOS [1]. Fission products were introduced into the integrated skimmer-ion source of the separator with a gas jet and cesium was ionized selectively in a surface ionization source at fairly low temperature (1100 °C). The beam of ^{142}Cs or ^{143}Cs was intercepted and the γ-rays emitted from the Cs-isotopes in equilibrium with their Ba-daughters were measured on line. The γ-ray line intensities were related to the known values of ^{142}La [2] and ^{143}Ce [3] measured off line after decay of their precursors.

The results are shown in Table I and may be compared to relative line intensities given in the literature [2,4]. Contradictory values of the half life of ^{143}Ba (20 s [5] and 14.5 s [6]) led us to remeasure this value. The decay of the strongest γ-rays of a mass separated sample of ^{143}Ba produced in a short (pulse) irradiation was followed over a time period of 130 s. The analysis of the decay curves gave a value for the half life of ^{143}Ba of

$$T_{1/2} = 17.0 \pm 0.8 \text{ s} \quad .$$

References

[1] A.K. Mazumdar, H. Wagner, G. Krömer, W. Walcher, M. Brügger, E. Stender, N. Trautmann, T. Lund, Nucl. Instr. Meth. 174 (1980) 183

[2] J.T. Larsen, W.L. Talbert, Jr., J.R. McConnell, Phys. Rev. C3 (1971) 1372

[3] M.A. Ludington, D.E. Raeside, J.J. Reidy, M.L. Wiedenbeck, Phys. Rev. C4 (1971) 647

[4] F. Schussler, J. Blachot, E. Monnand, B. Fogelberg, S.H. Feenstra, J. van Klinken, G. Jung, K.D. Wünsch, Z. Physik A290 (1979) 359

[5] T. Tamai, J. Takada, R. Matsushita, Y. Kiso, Inorg. Nucl. Chem. Lett. 9 (1973) 973

[6] J.C. Pacer, J.C. Hill, D.G. Shirk, W.L. Talbert, Phys. Rev. C17 (1980) 710

Table I. γ-ray line intensities in chains 142 and 143

a) Chain 142

Nuclide	E_γ(kev)	I_γ^{rel} % [2]	I_γ^{rel} % [this work]	I_γ^{abs} % [this work]
Cs	359.5	100	100	28.1 ± 2.8
Cs	966.9	36.5	33.1	9.3 ± 0.9
Cs	1175.9	11.9	15.3	4.3 ± 1.4
Cs	1423.0	8.0	6.8	1.9 ± 0.2
Cs	1333.1	5.0	7.5	2.1 ± 0.3
Ba	255.1	100	100	20.7 ± 2.1
Ba	894.9	61.5	60.9	12.6 ± 0.9
Ba	231.5	57.2	54.1	11.2 ± 0.9
Ba	948.8	50.0	45.9	9.5 ± 1.0
Ba	1078.5	52.2	55.1	11.4 ± 1.0
Ba	1000.9	44.0	51.2	10.6 ± 1.1
Ba	425.0	27.5	27.5	5.7 ± 0.7
Ba	363.8	22.2	20.3	4.2 ± 1.0
La	641.2 keV	I_γ^{abs} = 49.01 % [2] Reference line		

b) Chain 143

Nuclide	E_γ(kev)	I_γ^{rel} % [4]	I_γ^{rel} % [this work]	I_γ^{abs} % [this work]
Cs	195.0	100	100	12.2 ± 1.9
Cs	232.3	75	78	9.6 ± 0.9
Cs	306.4	52	55	6.7 ± 1.2
Cs	272.8	30	31	3.8 ± 0.5
Cs	534.8	10	10	1.2 ± 0.2
Cs	729.3	10	12	1.4 ± 0.3
Ba	211.5	100	100	24.0 ± 2.9
Ba	798.7	58	61	14.6 ± 1.5
Ba	1010.7	40	34	8.2 ± 0.9
Ba	925.2	18	15	9.7 ± 0.8
Ba	719.0	16	13	3.2 ± 0.3
Ba	435.7	8.2	7	1.6 ± 0.4
Ba	765.0	5.7	5	1.2 ± 0.2
Ce	293.3 keV	I_γ^{abs} = 41.3 % [3] Reference line		

INSTITUT FUER KERNCHEMIE

PHILIPPS-UNIVERSITAET MARBURG

1. Gamma-Ray Catalog

U. Reus, W. Westmeier, I. Warnecke[+]

Quantitative information on gamma rays from the decay of radioactive nuclides is required in many areas of nuclear science as well as related fields. We have therefore produced a compilation of the decay properties of all known radionuclides, with the main emphasis on energies and absolute intensities of gamma rays. A first printed version of this catalog was issued in 1979, covering references to the literature through June 1978.

Revision of data for a second issue has now been completed, and includes references through December 1981. The updated version contains information on ca. 2400 nuclides and isomers with a total of about 40.000 gamma rays, and additional information on X-ray emission has been introduced. As before, the catalog will be presented in two parts: In PART I gamma rays are listed in order of increasing energy for the purpose of identification of unknown gamma lines. In PART II complete data-sets for each nuclide are listed in order of mass number A and nuclear charge Z of the nuclides. This part also contains additional information, references, and comments in case of any discrepancies.

Though some computer work is still to be done, the second issue of the catalog will be completed soon. Publication is envisaged in an appropriate journal to ensure availability to all interested researchers.

2. Alpha-Energy Table

W. Westmeier, R. A. Esterlund

A compilation of alpha-decay properties of all known alpha-emitting nuclides, which includes data on alpha energies, intensities, and the abundance of the alpha branch, is permanently being updated. The table is ordered by increasing energy and covers data on 534 alpha emitters with a total of 1621 energies at present.
Computer printout copies of the table are available on request.

[+]Physikalisch-Technische Bundesanstalt, Braunschweig

Reaktorstation Garching; Fachbereich Physik
Technische Universität München

1. Coherent Neutron Scattering Lengths

L.Koester, K.Knopf, G.Reiner, W.Waschkowski

In continuation of the experiments for the determination of neutron scattering lengths b for the bound atoms of separated isotopes or single isotope elements we performed measurements on isotopically enriched compounds of the elements Zn, Ho, Tm, Yb and Lu.

By means of the Christiansen filter technique [1] we obtained the following preliminary data:

$b(^{64}Zn) = 5.23 \pm 0.10$ fm
$b(^{66}Zn) = 6.01 \pm 0.12$ fm
$b(^{67}Zn) = 7.64 \pm 0.15$ fm
$b(^{68}Zn) = 6.05 \pm 0.12$ fm
$b(^{nat}Zn) = 5.71 \pm 0.02$ fm
$b(^{170}Yb) = 6.77 \pm 0.10$ fm
$b(^{171}Yb) = 9.66 \pm 0.10$ fm
$b(^{172}Yb) = 9.43 \pm 0.10$ fm
$b(^{173}Yb) = 9.56 \pm 0.10$ fm
$b(^{174}Yb) = 19.2 \pm 0.2$ fm
$b(^{176}Yb) = 8.72 \pm 0.1$ fm
$b(^{nat}Yb) = 12.40 \pm 0.10$ fm

High precision experiments were carried out using the gravity refractometer [1]. Neutron reflection measurements on mirrors of molten thallium and liquid gallium result in preliminary values as follows:

$b(Tl) = 8.785 \pm 0.010$ fm and
$b(Ga) = 7.288 \pm 0.010$ fm.

The uncertainty of these results is mainly due to the uncertainty as given for the physical density of the molten probes . Experiments for the determination of these data are in progress.

2. Neutron Cross Sections

L.Koester, W.Waschkowski, K.Knopf

For the determination of the fundamental spin state scattering lengths two measured quantities are necessary such as values for the coherent scattering lengths b and for the scattering cross section σ_o at zero energy. Values for σ_o can be derived from total cross sections at eV-neutron energies taking into account the absorption cross section $\sigma_a(E)$ and in some cases an energy dependent resonance contribution $\sigma_r(E)$.

In order to obtain σ_o transmission measurements on solid or pulverized probes were performed at neutron energies of 1.26 eV and 5.19 eV and at 0.5 meV neutron energy for the determination of σ_a. Measurements on solid probes of the ordinary elements led to the following results for the total cross sections:

Zn: $\sigma_t(0.5meV) = 7.9 \pm 0.1$ b
$\sigma_t(1.26eV) = 4.203 \pm 0.010$ b
$\sigma_t(5.19eV) = 4.114 \pm 0.007$ b

Ga: $\sigma_t(0.5meV) = 20.0 \pm 0.2$ b
$\sigma_t(1.26eV) = 7.583 \pm 0.005$ b
$\sigma_t(5.19eV) = 7.091 \pm 0.006$ b

Se: $\sigma_t(1.26eV) = 9.495 \pm 0.010$ b
$\sigma_t(5.19eV) = 8.295 \pm 0.017$ b

Tl: $\sigma_t(1.26eV) = 10.50 \pm 0.02$ b
$\sigma_t(5.29eV) = 10.24 \pm 0.03$ b

Taking into account the results of the scattering lengths experiments values for σ_a, σ_o and for the total incoherent scattering cross section σ_i (all for free atoms) are obtained as follows:

Zn: σ_a(thermal) = 1.11 ± 0.02 b;
σ_o = 4.06 ± 0.02 b; σ_i = 0.073 ± 0.008 b.

Ga. σ_a(thermal) = 2.79 ± 0.06 b
σ_o = 7.03 ± 0.03 b; σ_i = 0.46 b.

Tl: σ_o = 10.01 ± 0.05 b; σ_i =0.17 ± 0.03 b.

References:

[1] L.Koester, Neutron scattering Lengths and Fundamental Neutron Interactions.
Springer Tracts in Modern Physics, Vol. 80, pp1-55
Berlin, Heidelberg, New York: Springer 1977

INSTITUT FÜR KERNENERGETIK UND ENERGIESYSTEME (IKE)
UNIVERSITÄT STUTTGART

The activities of the IKE in the fields of nuclear cross section data are extending to the generation or making available of evaluated nuclear cross section libraries and multigroup cross section informations for neutron and photon interaction and photon production. The mainly ENDF/B based data are needed for solving problems in the fields of reactor technology (reactor design, reactor safety), radiation protection and biomedical applications. The work is supported by BMFT via Fachinformationszentrum Energie, Physik, Mathematik GmbH in Karlsruhe. Some highlights of activities during 1981 are listed below.

1. Intercomparison of Evaluations of Actinide Neutron Nuclear Data

M. Mattes

Detailed comparisons of different evaluations for actinide isotopes from INDL/A /1/ and ENDF/B-V /2/ show discrepancies in the plotted cross sections and the calculated reaction rates for standard benchmarks, where the INDL/A data proved better agreement with the experimental values. In connection with this intercomparison, for Am-241 a format transfer of cross sections from UKNDL to ENDF/B-V was generated.

References

/1/ INDL/A IAEA Actinides Nuclear Data Library
/2/ ENDF/B Summary Documentation, BNL-NCS-17541, (ENDF-201) (1979)

2. Neutron Multigroup Library RESBIB-8500

M. Mattes, J. Keinert, W. Speyer

To consider the extremely varying cross sections of important resonance absorbers a multigroup energy structure below 4.703 keV with 8500 energy groups in the epithermal energy range was generated. The group cross sections are calculated for 6 temperatures in the temperature range from 300 K to 3000 K. Data bases for the RESBIB-8500 cross sections are ENDF/B-V and ENDF/B-IV. Presently, the library contains the most important fuel isotopes and in addition some neutron control absorbers. An IKE report is in preparation.

3. Thermal Neutron Cross Section Activities

3.1 Neutron scattering dynamics of polyethylene and paraffin, generation of cross section data for THERM-126

J. Keinert

For the thermal neutron multigroup cross section library THERM-126, the approved phonon spectrum model /1/ was applicated to calculate cross section data including scattering matrices for hydrogen bound in polyethylene/paraffin at room temperature. As a validity check differential and integral cross sections are compared with experimental data and several polyethylene/paraffin benchmarks are recalculated /2/.

3.2 Re-evaluation of the IKE Phononspectrum Model for Heavy Water and Generation of THERM-126 Cross Section Data

In providing THERM-126 with cross section matrices for deuterium bound in heavy water the IKE phonon spectrum /1/ was reevaluated. The changes /3/ are modifications in the acoustic part (hindered rotations and translations of the deuterium atom) and in the frequency of the upper oscillator, which is expected to be $1/\sqrt{2}$ of the value for the oscillator energy of H bound in H_2O. Contrary to the phonon spectrum model for D in D_2O in ENDF/B /4/ the band of hindered rotations in our model is assumed to be temperature dependent taking into account the diffusive motion of the D_2O-molecule. Thereby our model corresponds to a modified Haywood - Page model /5/.

With our new model scattering law data $S(\alpha,\beta)$ are generated in the temperature range 293.6 K - 673.6 K and then the cross section sets are calculated for THERM-126. In addition, a lot of differential and integral cross sections are compared to experimental values and benchmarks are recalculated /3/.

3.3 Compilation of Thermal Neutron Scattering Cross Sections for Hydrogen Bound in Moderators

For the moderator materials water, heavy water, polyethylene and the metal hydrides of zirconium and yttrium differential and integral point data scattering cross sections are compiled for room temperature and light water reactor working temperature /6/. In addition the bound hydrogen cross

sections are compared to the free gas approximation. The compilation contains physical highlights (dynamics of the molecules, phonon spectra), plotted differential and integral scattering cross sections and tabulated values for the considered initial and final neutron energies.

References

/1/ J. Keinert, IKE 6-89 (1975)

/2/ J. Keinert, IKE 6-136 (1981)

/3/ J. Keinert, IKE report in preparation

/4/ ENDF/B-IV Scattering Law Data, MAT = 1004, Tape 320, BNL

/5/ B.C. Haywood, D.I. Page, Neutron Thermalization and Reactor Spectra, Vol. 1, IAEA (1968)

/6/ J. Keinert, PHYSIK DATEN, 23-1 (1982)

4. Adjustment of Neutron Multigroup Cross Sections with Error Covariance Matrices to Deep Penetration Integral Experiments

G. Hehn, R.-D. Bächle, G. Pfister, M. Mattes, W. Matthes[+]

Radiation damage and shielding problems require special multigroup data libraries for treatment of neutron and gamma radiation in deep penetration of materials. The special features of group data for radiation shielding have ever profited by measurements of integral experiments. Modern adjustment of group cross section libraries can make use of the following important advantages:

a) the availability of comprehensive sensitivity studies showing the details of data requirements needed

b) the availability of error covariance information with correlation across energy range and reaction type, and last not least

c) the available results of clean deep penetration integral experiments designed for single materials in nearly onedimensional geometry.

Mainly because of the quadratic addition rule of errors, the biggest error contribution dominates over all smaller portions drastically, so that the need for adjustment of group cross sections and error covariance matrices is confined to very few elements with iron as the most important one. Within the modular code system RSYST an iterative adjustment procedure ADJUST-EUR

has been established, using one- and twodimensional S_N-calculation with linear perturbation theory. The deep penetration iron experiment ASPIS/ Winfrith was reevaluated with new error covariance data available and first measurements of the integral experiment EURACOS/Ispra have been used additionally.

The data adjustment is performed in 100 neutron groups and supplied with the appropriate covariance matrices in the EURLIB-5 library for coupled neutron and gamma calculations. The iron integral experiments were evaluated with a special super-fine group structure between 3 MeV and 20 keV to cover the neutron streaming along the cross section minima in the large iron blocks. We got there a proper resonance weighting for the EURLIB group data locally dependent from the penetration depth. The adjustment needed for the group data can be explained as correction to the weighting function primarily, and secondly as an effective reduction of energy degradation by the inelastic scattering process of iron.

+ CCR Euratom, Ispra / Italy

INSTITUT FÜR STRAHLENPHYSIK

UNIVERSITÄT STUTTGART

Experiments With Polarized Neutrons

G. Bulski, W. Grum, J. W. Hammer, H. Postner, G. Schleußner

1. Analyzing Power of ^{12}C, ^{209}Bi, Pb, Cu, And Some Other Nuclei

14 angular distributions of analyzing power have been measured, especially at about 7.7MeV n-energy. Polarization of the $^{9}Be(\alpha,n)^{12}C$-neutrons is high in this region (40-60%).

Carbon-12 has been investigated at 5 different energies, also measurements with 3 sample sizes have been carried out. The aim of the Carbon-12 measurements was to get a revision of the accuracy of the method used by us and to establish a method for finite geometry corrections. For doing these corrections we used the Monte Carlo-code JANE by E.Woye /1,2/, which also allows to calculate the polarization of multiple scattered neutrons. Fig. 1 shows the result of the analyzing power measurement of Carbon-12 for 3 sample sizes after corrections for finite geometry effects, Figs 2-6 show the analyzing power of Carbon-12 at the n-energies 7.55, 7.65, 7.85, 8.05, and 8.73MeV. The strong energy dependance is due to resonances in this energy region, the energy spread of the neutrons was 160keV. In opposition to ^{12}C, where only Monte Carlo-methods can be applied for calculating the corrections, one can use also analytical methods /2/ for heavy nuclei like ^{209}Bi. The result of the experiment is shown in Fig. 7.

Because of some discrepancies between experiment and optical model calculations especially for Lead and Copper /3/ we measured the analyzing power at the lower energy 7.7MeV. Figs 8 and 9 show the result of these measurements and no abnormity at small angles can be seen. With our improved method we remeasured the analyzing power of natural Lanthanum and Uranium-238.

The optical model calculations (coupled channels calculations) for all nuclei involved are not yet completed.

2. Differential Cross Section Data

For all analyzing power measurements a differential cross section can be evaluated in relative units. Fig. 10 shows the result for ^{209}Bi with corrections made by analytical methods, therefore no data points can be shown. Preparation of our unfolding code to get absolute data is in progress.

3. Improvements Of Experimental Setup And Evaluation

The detectors used have been improved by better magnetic shielding and optimized light guides according to /4/. Also monitoring the neutron flux has been improved using scintillation detectors as monitors. Back ground could be reduced by a factor of about 3 applying additional shielding. The accuracy of the analyzing power measurements has been improved drastically by switching the spin every five minutes and storing the data simultaneously for both spin states. Essential parts of the unfolding procedure for the proton recoil spectra are and will be coded new. Digital filtering using the Fast Fourier Transform method /5/ improved the results of the unfolding procedure. Figs 11 and 12 show the unfolded neutron spectra for the both spin states for Si at two scattering angles. The peaks of elastic and inelastic scattering can clearly be distinguished and evaluated.

The unfolding procedure will further be improved by using a more accurate response matrix for the detectors. The response matrix has been calculated using the code NRESP4 by G. Dietze /6/.

Data handling has been managed using a Z80-based microcomputer system, all calculations have been done on the Cyber174 in the University Computer Center.

4. Activities Still In Progress

Analyzing power and differential cross section will be measured for the nuclei Ca, Si, S, W, and Th.

5. These investigations have been made without any financial support from outside the university.

6. References

/1/ E. Woye, Tübingen, Code JANE, private communication

/2/ W. Grum, Diplomarbeit, Stuttgart (1981)

/3/ R. B. Galloway and A. Waheed, Phys. Rev. C19 (1979) 268

/4/ H. Klein and H. Schölermann, Improvement of the light collection in scintillation detectors, IEEE Trans. Nucl. Sci. (1978)

/5/ T. Inouye et al., Nucl. Instr. Meth. 67 (1969) 125

/6/ G. Dietze, PTB Braunschweig, Code NRESP4, private communication

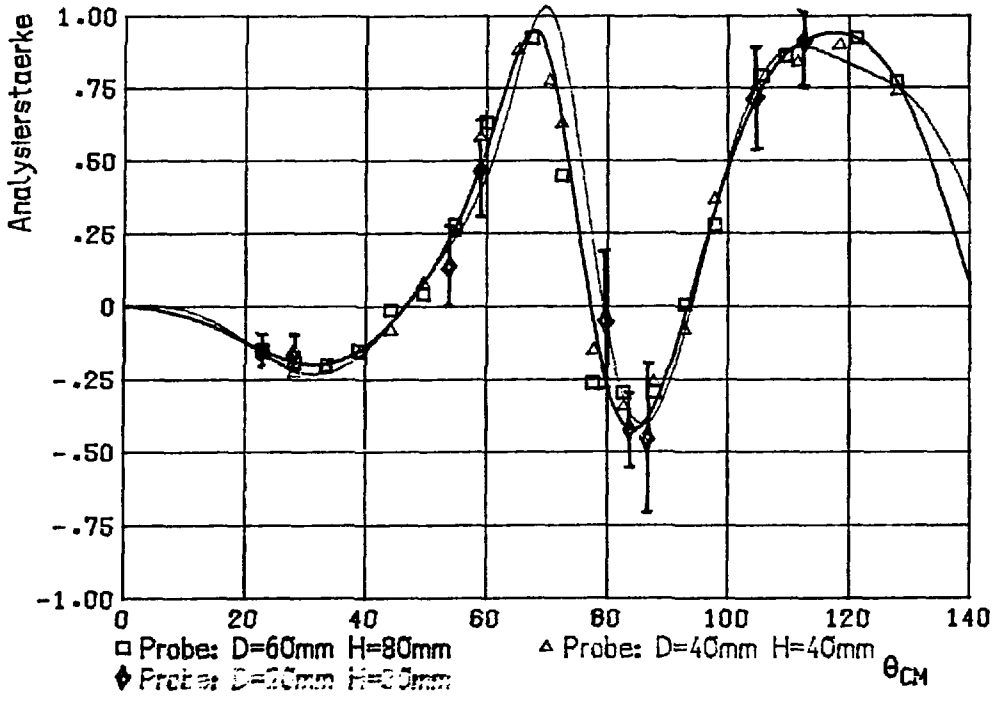

Fig. 1 Analyzing power of Carbon-12 for E_n=7.65MeV using 3 different sample sizes with finite geometry corrections

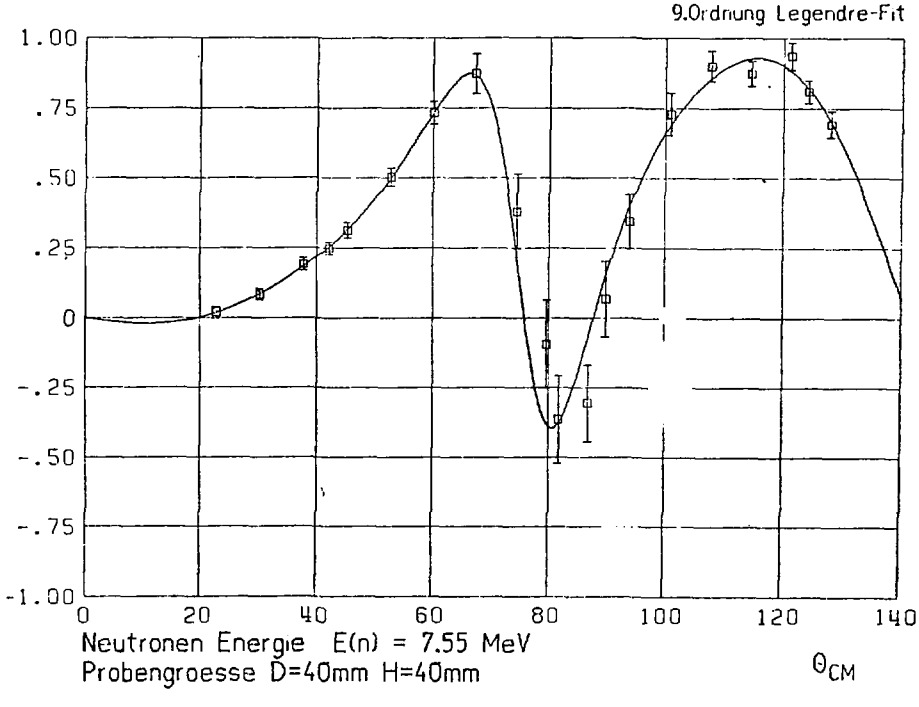

Fig. 2 Analyzing power of Carbon-12 with finite geometry corrections E_n=7.55MeV

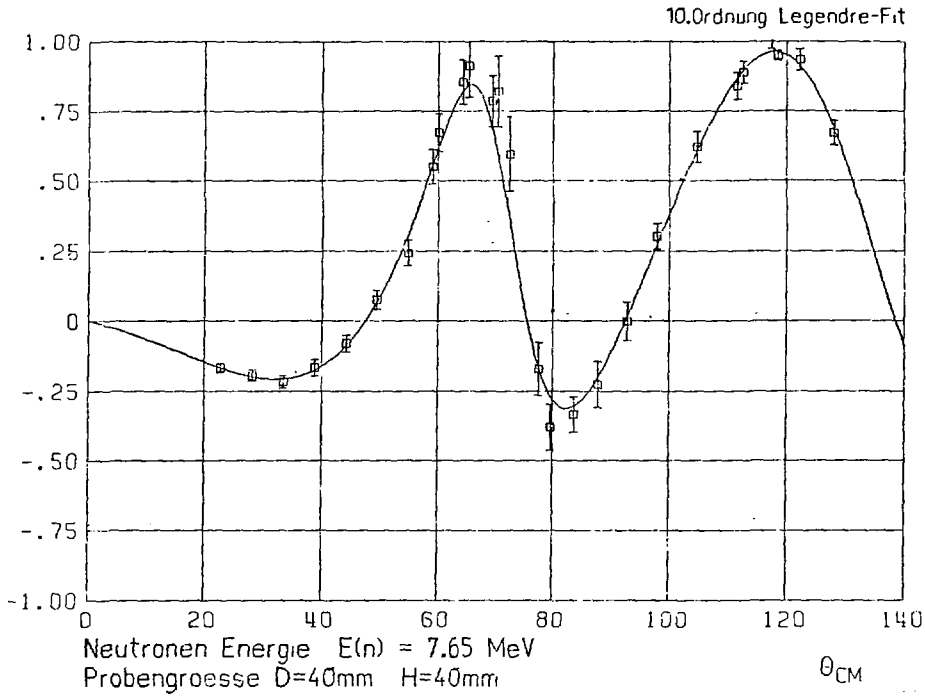

Fig. 3 Analyzing power of Carbon-12 with finite geometry corrections E_n=7.65MeV

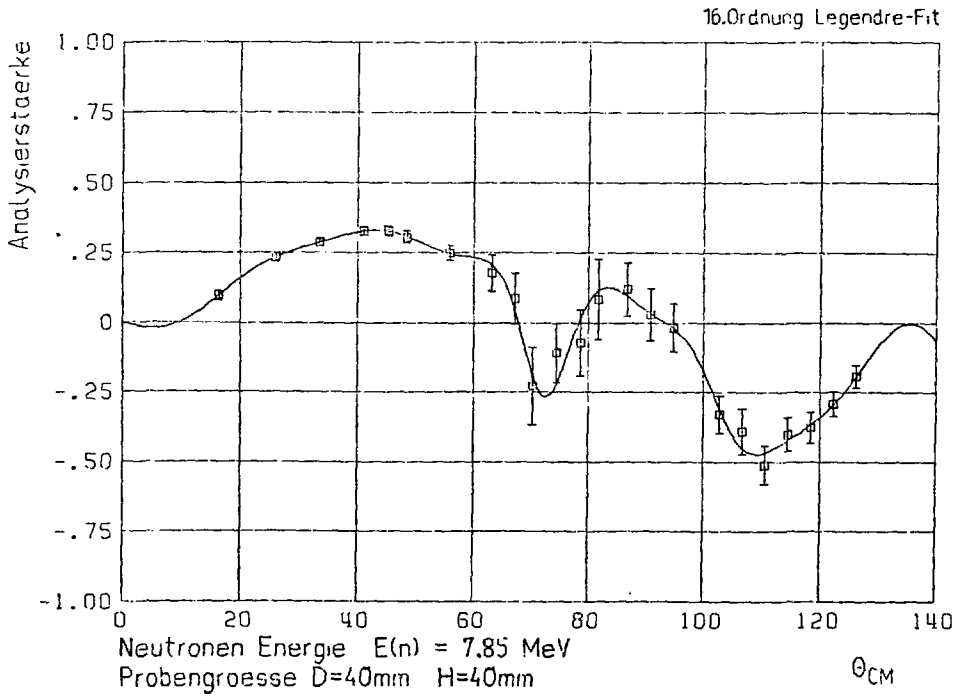

Fig. 4 Analyzing power of Carbon-12 with finite geometry corrections E_n=7.85MeV

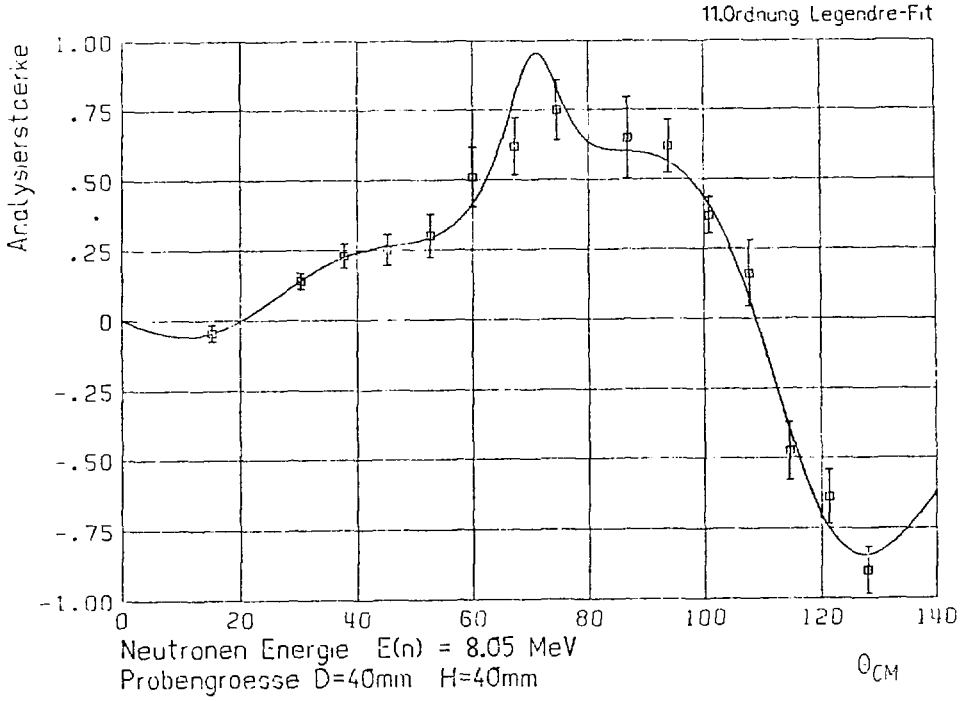

Fig. 5 Analyzing power of Carbon-12 with finite geometry corrections E_n=8.05MeV

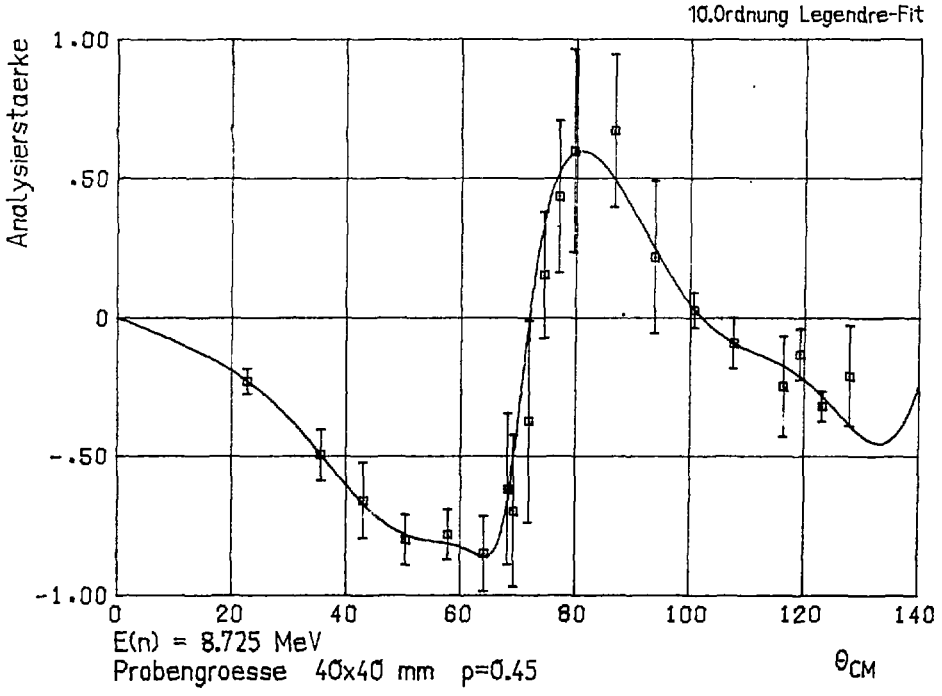

Fig. 6 Analyzing power of Carbon-12 without finite geometry corrections, E_n=8.73MeV

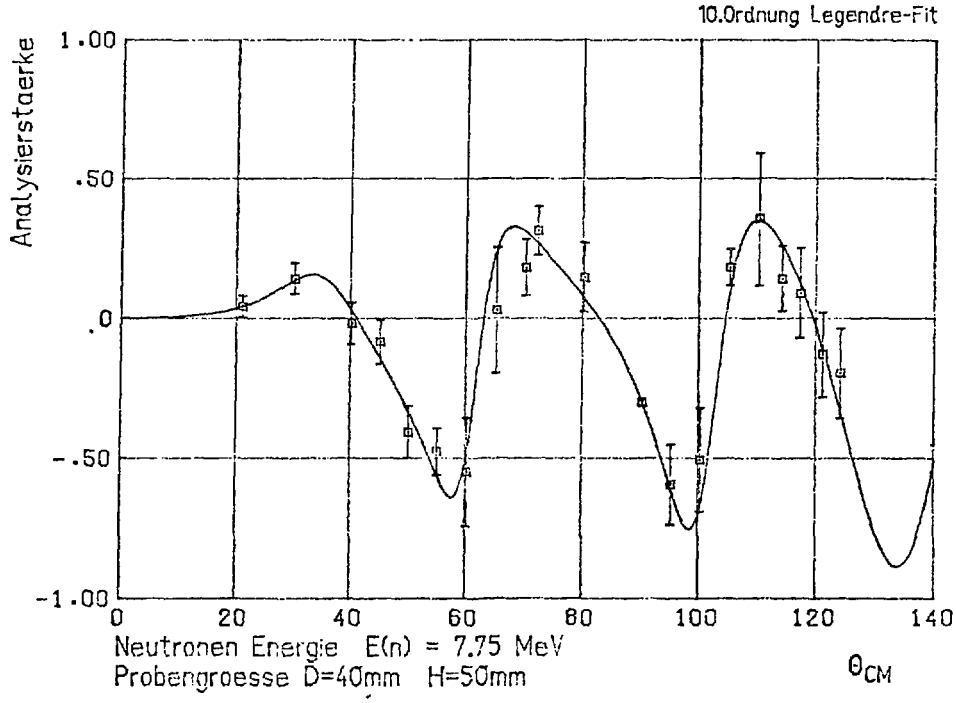

Fig. 7 Analyzing power of ^{209}Bi at E_n=7.75MeV

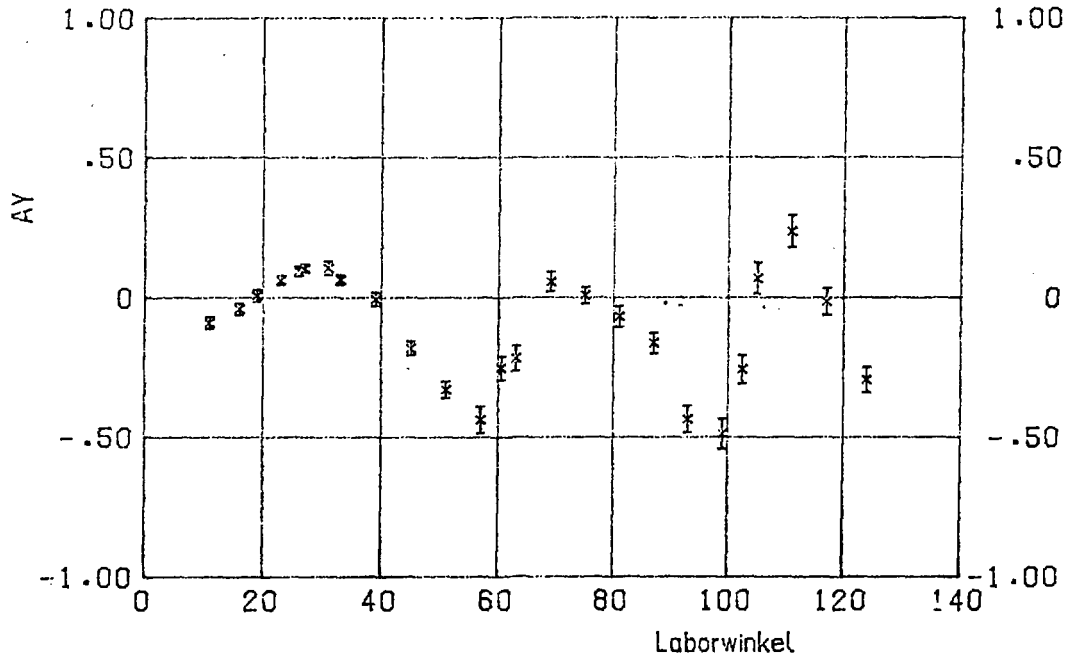

Fig. 8 Analyzing power of natural lead at E_n=7.75MeV
uncorrected data

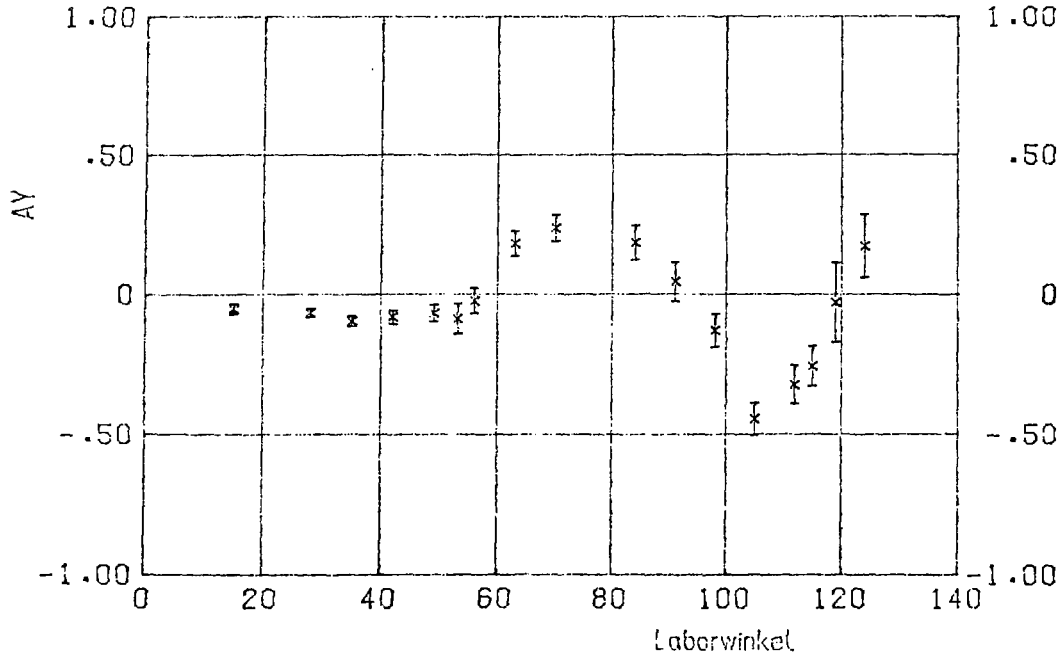

Fig. 9 Analyzing power of natural copper at E_n=7.75MeV uncorrected data

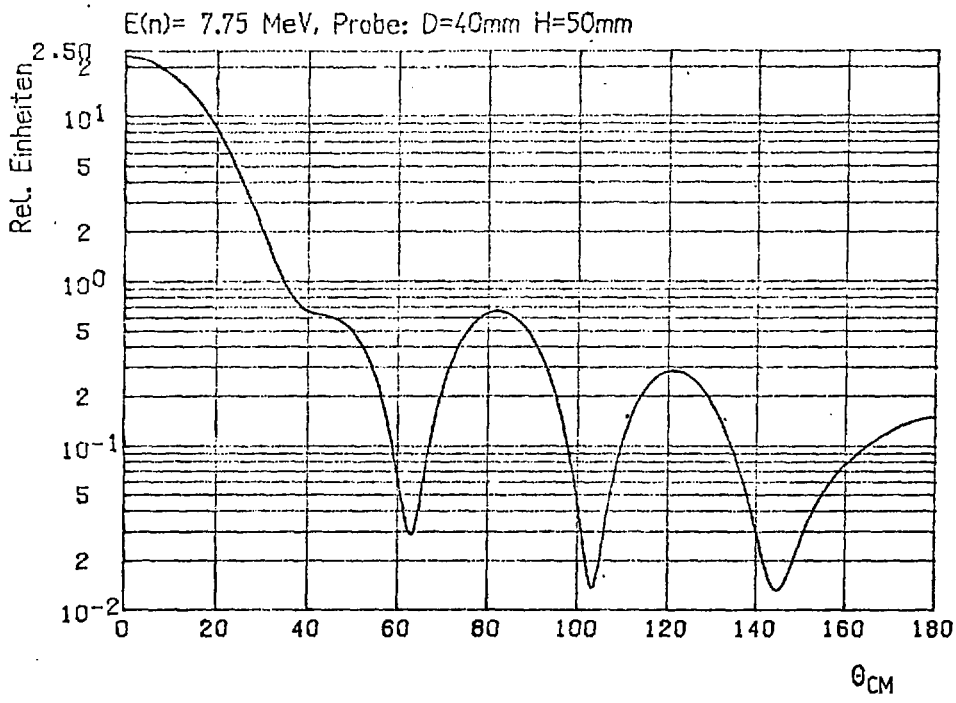

Fig. 10 Relative differential cross section of ^{209}Bi at E_n=7.75MeV

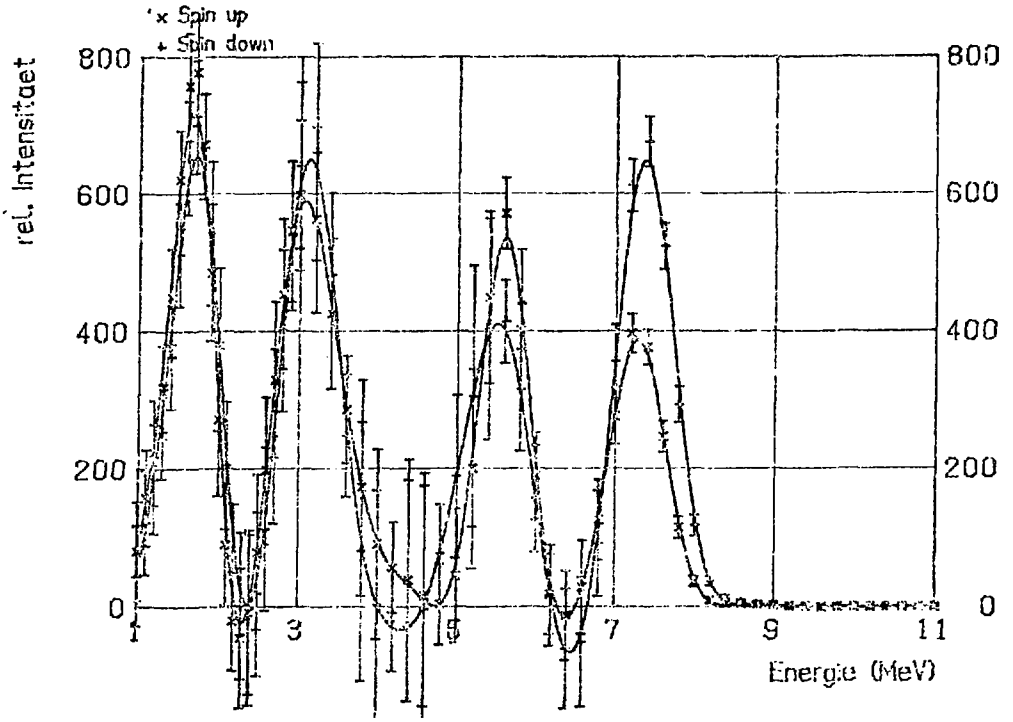

Fig. 11 Unfolded proton recoil spectra for 7.75MeV neutrons scattered by Si at 96°, elastic and inelastic peak well separated

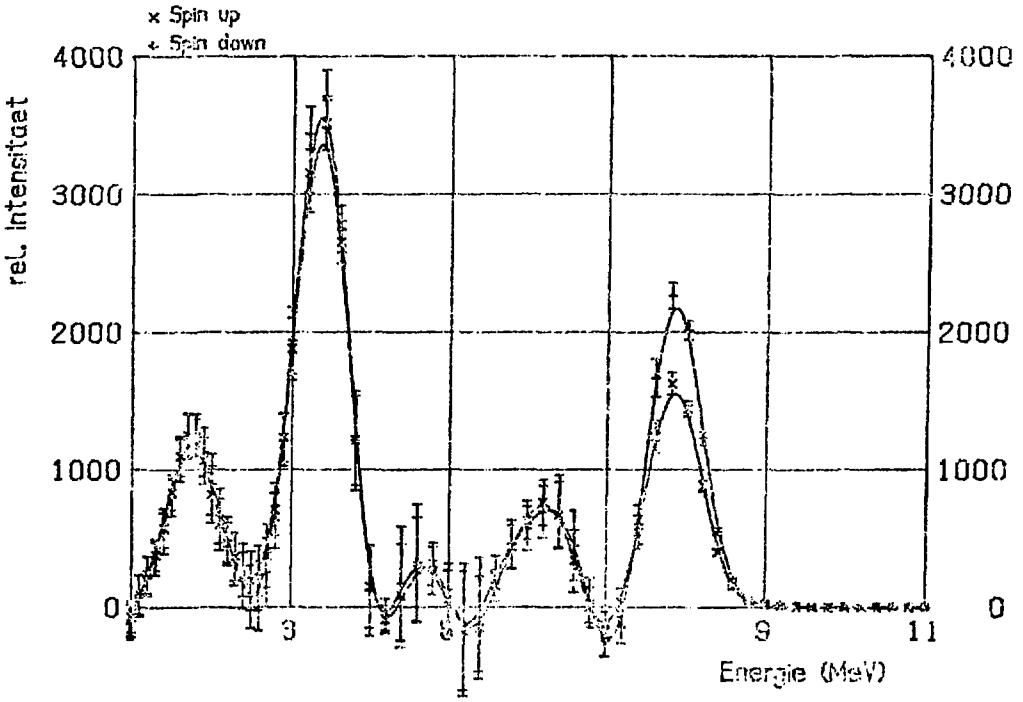

Fig. 12 Unfolded proton recoil spectra for 7.75MeV neutrons scattered by Si at 42°, elastic and inelastic peak well separated

PHYSIKALISCH-TECHNISCHE BUNDESANSTALT
BRAUNSCHWEIG

1. Radionuclide Data

1.1 Half-Lives

K.F. Walz, U. Schötzig

Half-lives of some long-lived radionuclides were determined by following the decay of encapsulated sources with a high pressure 4πγ ionisation chamber and/or a Ge(Li)-spectrometer. The results are summarized in Table I. Uncertainties (in brackets) correspond to one standard deviation. The measuring period t is given a ratio to the half-life $T_{1/2}$. A 0.4 % ^{154}Eu impurity in ^{152}Eu was accounted for. In the Ge(Li) measurements the full energy peaks at 105 keV (^{155}Eu), 123 keV and 1274 keV (^{154}Eu) of a mixed ^{154}Eu/^{155}Eu spectrum were analysed.

1.2 Gamma-Ray Emission Probabilities

K. Debertin, U. Schötzig

Gamma-ray emission probabilities p of ^{226}Ra in equilibrium with its daughter products and of some radionuclides emitting low energy gamma-radiation were determined by using sources of known activity and calibrated Ge(Li) and high purity germanium spectrometers. The results are summarized in Table II. Uncertainties (in brackets) correspond to one standard deviation.

1.3 X-Ray Emission Probabilities of ^{93}Nb^{m}

W. Peßara

Emission probabilities p for the X_K-radiation from ^{93}Nb^{m} were determined by using a well-calibrated high-purity germanium detector. The efficiency curve in the energy region

from 6 to 36 keV was established using the X_K-radiations of the nuclides ^{57}Co, ^{65}Zn, ^{85}Sr, ^{88}Y, ^{109}Cd and ^{125}I and the gamma radiations from ^{241}Am and ^{125}I.

The $^{93}Nb^m$ sources were produced by drying (on VYNS foils) weighed drops of a solution of known specific activity determined by CBNM Geel with the liquid scintillation method. The following results were obtained:

$$p_K = 0.107 \pm 0.003$$
$$p_{K_c} = 0.0892 \pm 0.0025$$
$$p_{K_\beta} = 0.0174 \pm 0.0005$$
$$p_{K_\beta}/p_{K_c} = 0.195 \pm 0.001$$

The uncertainties correspond to one standard deviation.

Table I. Half-lives

Nuclide	$t/T_{1/2}$	$T_{1/2}$ (ionis.ch.)	$T_{1/2}$ (GeLi)
Kr-85	0.3	10.74(4)a	-
Ba-133	0.6	10.53(4)a	-
Eu-152	0.5	13.53(3)a	-
Eu-154	0.4	8.59(2)a	8.54(5)a
Eu-155	0.8	-	4.67(2)a

Table II. Gamma-ray emission probabilities

Nuclide	Energy in keV	p
Ra-226	186.0	0.0351(6)
	241.9	0.0712(11)
	295.2	0.182(3)
	351.9	0.351(4)
	609.3	0.446(5)
	768.4	0.0476(7)
	934.0	0.0307(4)
	1120.3	0.147(2)
	1238.1	0.0578(7)
	1509.2	0.0208(5)
	1764.5	0.151(3)
	2118.5	0.0117(3)
	2204.1	0.0498(12)
	2447.7	0.0155(4)
Am-241	26.4	0.0241(5)
I-125	35.5	0.0651(13)
Pb-210	46.5	0.0418(9)
Ag-108m	79.2	0.0579(17)
I-131	80.2	0.0265(5)

2. Neutron cross sections

2.1 Fission spectrum-averaged neutron cross section of the reaction $^{93}Nb(n,n')^{93}Nb^{m}$

W.G. Alberts

In the framework of measuring ^{252}Cf spontaneous fission neutron spectrum-averaged cross sections for reactions used in reactor metrology the niobium activation detector was investigated. Metallic samples of 28 µm thickness were irradiated close to the ^{252}Cf neutron source of the PTB in an open air facility /1/. Indium foils were attached to measure the neutron fluence. The activity of the isomer $^{93}Nb^{m}$ was determined relative to an activity standard considering geometry and self-absorption corrections. Based on a spectrum- averaged cross section of (195 ± 5) mb for $^{115}In(n,n')^{115}In^{m}$ we obtained a cross section of (149 ± 10) mb /2/ which is in good agreement with a value of (158 ± 16) mb obtained from averaging a recently published calculated cross section /3/ over the ^{252}Cf neutron spectrum.

/1/ W. Mannhart, W.G. Alberts, Nucl.Sci.Eng. 69 (1979) 333

/2/ W.G. Alberts, R. Hollnagel, K. Knauf, M. Matzke, W. Peßara, Proc. 4th ASTM-EURATOM Symposium on Reactor Dosimetry, Gaithersbourg, Md., 1982, to be published

/3/ B. Strohmaier, S. Tagesen, H. Vonach, Physik-Daten - Physics Data 13 (1980) 62.

3. Variable Energy Cyclotron and Fast Neutron TOF-Spectrometer

The PTB-multi-angle time-of-flight (TOF) spectrometer has been used to study the $^{12}C(n,\alpha)^{9}Be$, $^{12}C(n,n)$ and $^{12}C(n,n')$ cross sections and to measure neutron spectra from ^{252}Cf and from the bombardment of thick Be targets with deuterons. Further investigations were aimed at a precise determination of the efficiency of the scintillation detectors.

3.1 Differential cross section of $^{12}C(n,\alpha_0)^{9}Be$

H.J. Brede, G. Dietze, H. Klein and H. Schölermann

From response function measurements with an NE 213 scintillation detector, 5 cm thick and 5 cm in diameter, the differential cross section of the reaction $^{12}C(n,\alpha_0)^{9}Be$ has been determined for neutron energies from 8 to 10 MeV. The method consisted of an accurate comparison of the measured spectrum produced by the incident monoenergetic neutrons with a response spectrum calculated by the Monte-Carlo code NRESP4 /1/. The pulse height distribution induced by the $^{12}C(n,\alpha_0)^{9}Be$ reaction within the scintillator could be separated. This distribution corresponds to the energy distribution of the α-particles which is directly correlated to their angular distribution. A set of Legrende-coefficients has been determined for the differential cross section of $^{12}C(n,\alpha_0)^{9}Be$ in the center of mass system.

3.2 Fast Neutron Scattering on Natural Carbon and Polyethylen Energy Range 6 MeV $\leq E_n \leq$ 14 MeV

R. Böttger, H.J. Brede, H. Klein, H. Schölermann, B.R.L. Siebert

First scattering experiments have been performed with the multi- angle neutron time-of-flight spectrometer. Various natural carbon and polyethylene samples were used to deter-

mine the elastic and inelastic cross section for neutron energies in the range of 6 MeV up to 14 MeV in steps of 1 MeV.

Sample size effects were extensively studied at E_n = 10 MeV. Preliminary analysed experimental data reasonably agree with full Monte-Carlo simulations.

The final analysis of the complete set of experimental data is in progress including the absolute scaling, the extraction of Legendre coefficients by means of the matrix-inversion method and the comparison with evaluated cross-sections (ENDF/B-V).

3.3 The Neutron Energy Spectrum from the Spontaneous Fission of ^{252}Cf in the Energy Range of 2 MeV $\leq E_n \leq$ 14 MeV

R. Böttger, A. Chalupka[+], H. Klein

An improved fast ionisation chamber with a low mass Au-capsule /2/ was used as timing detector to measure the neutron energy spectrum of the spontaneous fission of ^{252}Cf with the multi-angle time-of-flight spectrometer. At a mean fission rate of 10^5/s the chamber had excellent properties regarding the time resolution, the α-discrimination and the total efficiency.

Neutron TOF-spectra were recorded for about 320 h using four large volume liquid scintillators (5.07 cm x 25.4 cm Ø) simultaneously behind a flight path 12 m in length. The spectra had to be corrected for random background events as well as for uncorrelated stops and finally to be renormalised /3/.

The neutron detection efficiency of the liquid scintillators were calibrated in monoenergetic neutron fields using to a proton recoil telescope as an absolute fluence meter. The

[+] Institut für Radiumforschung und Kernphysik, Wien

calibration includes all distortions due to the liner material of the collimator and the air. Thus the neutron spectra could be compared with commonly used Maxwellian distributions on an absolute scale. The analysis is in progress.

3.4 Spectral neutron yield from a thick Be-target bombarded by 11.7 MeV deuterons

H.J. Brede, G. Dietze and D. Schlegel-Bickmann

The neutron energy spectrum from a Be-target, 2 mm thick, bombarded by 11.7 MeV deuterons from the cyclotron was measured using a 12.5 m flight path and a NE 213 scintillation detector, 5 cm thick and 5 cm in diameter. The spectral neutron yield was determined for neutron energies between 0.4 and 16 MeV at 0^{o}, 5^{o}, 10^{o}, 20^{0} and 30^{o} to the direction of the incident deuteron beam. The neutron spectral distribution changes strongly within this angular range. A peak at E_n = 0.8 MeV has been always obtained similar to the measurement of Lone et al. /4/.

3.5 Properties of Liquid Scintillation detectors

R. Böttger, H.J. Brede, G. Dietze, H. Klein, H. Schölermann, B.R.L. Siebert

Various liquid scintillation detectors, which are used as time-of-flight detectors or monitors in the multi-angle fast neutron spectrometer, were investigated with respect to the light output functions, the pulse height resolution and the neutron detection efficiency.

Recently evaluated angular distributions of the neutron producing reaction $D(d,n)^{3}He$ /5/ and a proton recoil telescope were applied to determine the detector response for monoenergetic neutrons in the energy range from 2 MeV up to 14 MeV.

Regarding the shape of the response spectra excellent agreement is achieved with Monte Carlo simulations (code NRESP4 /1/). Nevertheless, in the absolute scale, energy dependent deviations up to 10 % arise with respect to the fluence measured with the proton recoil telescope. This discrepancy will be subject of further investigations.

/1/ G. Dietze, PTB-Bericht ND-22 (1982)
/2/ A. Chalupka, Nucl. Instr. and Meth. 164 (1979), 105-112
/3/ A. Chalupka, Nucl. Instr. and Meth. 165 (1979), 103-108
/4/ M.A. Lone, A.J. Ferguson and B.C. Robertson, Nucl. Instr. and Meth. 189 (1981), 515-523
/5/ M. Drosg, Nucl. Sci. Eng. 67 (1978), 190-220

FACHINFORMATIONSZENTRUM ENERGIE PHYSIK MATHEMATIK

Status Report

H. Behrens, J.W. Tepel

1. Information System for Physics Data in the Federal Republic of Germany

This project has been deschribed earlier in the Progress Reports NEANDC (E) - 172 U Vol. V, NEANDC (E) - 182 U Vol. V and NEANDC (E) - 192 U Vol. V.No details are therefore given here.

2. New Data compilations

The following new issues in the series Physics Data were published in the meantime:

5-7 (1981): Gases and Carbon in Metals (Thermodynamics, Kinetics, and Properties).
Part VII: Group VA Metals (1): Vanadium (V)
G. Hörz, H. Speck, E. Fromm and H. Jehn

5-8 (1981): Gases and Carbon in Metals (Thermodynamics, Kinetics and Properties).
Part VII: Group VA Metals (2): Niobium (Nb)
G. Hörz, H. Speck, E. Fromm and H. Jehn

5-9 (1981): Gases and Carbon in Metals (Thermodynamics, Kinetics, and Properties).
Part IX: Group VA Metals (3): Tantalum (Ta)
G. Hörz, H. Speck, E. Fromm and H. Jehn

5-12 (1982): Gases and Carbon in Metals (Thermodynamics, Kinetics, and Properties).
Part XII: Group VII A Metals, Manganese, Technetium, Rhenium (Mn, Tc, Re).
H. Jehn, H. Speck, E. Fromm and G. Hörz

5-13 (1981) Gases and Carbon in Metals (Thermodynamics,Kinetics, and Properties).
Part XIII: Ferrous Metals (1): Iron-Hydrogen (Fe-H).
E. Fromm, H.Speck, H.Jehn and G. Hörz

5-14 (1981) Gases and Carbon in Metals (Thermodynamics, Kinetics, and Properties).
Part XIV: Ferrous Metals (2): Iron-Carbon (Fe-C).
E. Fromm, H.Speck, H.Jehn and G. Hörz.

5-15 (1982) Gases and Carbon in Metals (Thermodynamics, Kinetics, and Properties).
Part XV: Ferrous Metals (3): Iron-Nitrogen (Fe-N).
E. Fromm, H. Jehn, W. Hehn, H.Speck and G. Hörz.

11-2 (1981) Nucleon-Nucleon Scattering Data. Summary Tables (1981 Edition)
J. Bystricky and F. Lehar

11-3 (1981) Nucleon-Nucleon Scattering Data. Detailed Tables(Supplement 1).
J. Bysticky and F. Lehar

13-3 (1981) Evaluation of the Cross-Sections for the Reaction $^{27}Al(n,a)^{24}Na$.
S. Tagesen and H. Vonach.

16-2 (1981) The Homogeneous Framework of the Cubic Crystal Structures
E. Hellner, E. Koch and A. Reinhardt.

18-2 (1981): Optical Properties of Metals
Part II: Noble Metals, Aluminium, Scnadium, Yttrium, the Lanthanides and the Actinides (o,1 h 5oo eV)
(Cu, Ag,Au; Al;Sc;Y;La,Ce,Pr,Nd,Sm,Eu,Gd,Tb,Dy,Ho,Er,Tm, Yb,Lu; Th,U,Am).
J.H. Weaver, C. Krafka, D.W. Lynch and E.E. Koch XIV

21-1 (1982): Bibliography of Gas Phase Electron Diffraction. 193o-1979.
I. Buck, E. Maier, R. Mutter, U. Seiter, C. Spreter.
B. Starck, I. Hargittai, O. Kennard,D.G. Watson,A.Lohr,
T. Pirzadeh, H.G. Schirdewahn and Z. Majer XIV

22-1 (1981): Phenomenolocical Analyses of Nucleon-Nucleon Scattering
P. Kroll

23-1 (1982): Temperature Dependence of Thermal Neutron Scattering Cross Sections for Hydrogen Bound in Moderators.
J. Keinert.

3. Bibliographic of Existing Data Compilations

The corresponding database INKA-Datacomp has been once again updated in the meantime. A new completed printed issue of the whole bibliography is in preparation.

4. The Evaluated Nuclear Structure Data File

Evaluation work on the mass chain A = 98 has been completed. The mass chains A = 95 and 96 have recently been returned by the reviewer and should appear in print shortly. Work on the mass chains A = 97 and A = 93 is continuing, whereas evaluation on A = 94 and A = 82 has just started.

Considerable effort was undertaken in order to load ENSDF as ADABAS-files on our Siemens 7.76o Computer. Since ADABAS makes use of the relational model of data bank structures, the complex hierarchial relationships inherent in ENSDF had to be represented by in adding a special 19-digit key to each record. The original ENSDF-file was split into four different ADABAS-files logically coupled through this key. A retrieval system was built up by using the interactive query and pro-

gramming language. Special features mainly connected with string handling had to be programmed in ASSEMLER language. An ASSEMBLER interface was written in order to faciliate the analysis of data entered from the terminals and to pass back modified parameters to the ADABAS-system. Automatic conversion oftime units into seconds is one of the features of this system.

The bibliographic data base associated with ENSDF, the Nuclear Structure Reference File (NSR) as well as a file MEDLIST containing the radiation emitted from all unstable nucleides were transcribed into ADABAS-readable form. Both files are performing well under ADABAS with advantages mainly resulting from easy updating and data handling.

APPENDIX

Addresses of Contributing Laboratories

Institut für Angewandte Kernphysik II
Director: Prof.Dr. G. Schatz
Senior reporter: Dr. F. Käppeler
Kernforschungszentrum Karlsruhe
Postfach 3640
7500 Karlsruhe

Institut für Kernphysik II
Director: Prof.Dr. A. Citron
Senior reporter: Dr. S. Cierjacks
Kernforschungszentrum Karlsruhe
Postfach 3640
7500 Karlsruhe

Institut für Neutronenphysik und Reaktortechnik
Direktor: Prof.Dr. G. Kessler
Senior reporters: Dr. F.H. Fröhner
Dr. B. Goel
Kernforschungszentrum Karlsruhe
Postfach 3640
7500 Karlsruhe

Institut für Chemie (1): Nuklearchemie
Director: Prof.Dr. G. Stöcklin
Senior reporter: Dr. S.M. Quaim
Kernforschungsanlage Jülich
Postfach 1913
5170 Jülich

Institut für Reine und Angewandte
Kernphysik
Director: Prof.Dr. K.O. Thielheim
Senior reporter: Dr. H.G. Priesmeyer
Universität Kiel, Geesthacht
Reaktorstr. 1
2054 Geesthacht/Tesperhude

Institut für Kernchemie
Director: Prof.Dr. W. Herr
Senior reporter: Dr. R. Michel
Universität zu Köln
Zülpicher Str. 47
5000 Köln

Institut für Kernchemie
Director: Prof.Dr. G. Herrmann
Senior reporter: Prof.Dr. H.O. Denschlag
Universität Mainz
Fritz-Strassmann-Weg 2
6500 Mainz

Institut für Kernchemie
Senior reporter: Prof.Dr. P. Patzelt
Philipps-Universität Marburg
Lahnberge
3550 Marburg/Lahn

Fachbereich Physik der
Technischen Universität München
Abteilung E14, Forschungsreaktor
Head and senior reporter: Prof.Dr. L. Köster
8046 Garching/München

Institut für Kernenergetik und Energiesysteme
Director: Prof.Dr. K.H. Höcker
Senior reporter: Dr. J. Keinert
Universität Stuttgart
Pfaffenwaldring 31
7000 Stuttgart 80 (Vaihingen)

Institut für Strahlenphysik
Director: Prof.Dr. K.W. Hoffmann
Senior reporter: J.W. Hammer
Universität Stuttgart
Allmandring 3
7000 Stuttgart 80

Physikalisch-Technische Bundesanstalt
Abteilung 6, Atomphysik
Director: Prof.Dr. S. Wagner
Bundesallee 100
3300 Braunschweig

Fachinformationszentrum Energie, Physik, Mathematik
Directors: Dr. W. Rittberger, E.-O. Schulze
Senior reporter: Dr. H. Behrens
Kernforschungszentrum
7514 Eggenstein-Leopoldshafen 2

CINDA TYPE INDEX

A Supplement to Progress Report on
Nuclear Data Research in the Federal
Republic of Germany for the Period
April 1, 1980 to March 31, 1981

NEANDC(E)-222 U Vol. V
INDC (Ger)-23/L + Special
FIZ-KA-2

ELEMENT S	A	QUANTITY	TYPE	ENERGY MIN	ENERGY MAX	DOCUMENTATION REF	VOL	PAGE	DATE	LAB	COMMENTS
FP	ROD	TOTAL	EXPT-PROG	30+0	60+1	NEANDC(E)-232U	882	KIL		VOL.V.P.33	PRIESMEYER+ CS133/135/137
FP	ROD	TOTAL	EXPT-PROG	30+0	60+1	NEANDC(E)-232U	882	KIL		VOL.V.P.33	PRIESMEYER+ TRANS EXPT
MA	NY	THERMAL SCAT	EVAL-PROG	NDG		NEANDC(E)-232U	882	THS		VOL.5.P.54	KEINERT. THERM-126, NDG
H	PLE	TOTAL	EXPT-PROG	60+6	14+7	NEANDC(E)-232U	882	PTB		VOL.5.P.70	BOETTGER+ TOF EXPT, NDG
H	PLE	THERMAL SCAT	COMP-PROG	NDG		NEANDC(E)-232U	882	THS		VOL.5.P.54	KEINERT. SCAT SIG,NDG
H	WTR	THERMAL SCAT	COMP-PROG	NDG		NEANDC(E)-232U	882	THS		VOL.5.P.54	KEINERT. SCAT SIG, NDG
D	D2O	THERMAL SCAT	COMP-PROG	NDG		NEANDC(E)-232U	882	THS		VOL.5.P.54	KE.NERT. SCAT SIG,NDG
LI	007	N,N TRITON	EXPT-PROG	TR	80+6	NEANDC(E)-232U	882	JUL		VOL.V.P.28	LISKIEN+ SIG,EXCIT FN,NDG
C		ELASTIC SCAT	EXPT-PROG	60+6	14+7	NEANDC(E)-232U	882	PTB		VOL.5.P.70	BOETTGER+ TOF EXPT, NDG
C	012	N,ALPHA	EXPT-PROG	FAST		NEANDC(E)-232U	882	PTB		VOL.5.P.70	ALBERTS, TOF EXPT,NDG
C	012	N,ALPHA	EXPT-PROG	80+6	10+7	NEANDC(E)-232U	882	PTB		VOL.5.P.70	BREDE+ DIFF-SIG EXPT,NDG
C	012	POLARIZATION	EXPT-PROG	76+6		NEANDC(E)-232U	882	IFS		VOL.V.P.57	BULSKI+ ANALYZ POWER
C	012	POLARIZATION	EXPT-PROG	77+6		NEANDC(E)-232U	882	IFS		VOL.V.P.57	BULSKI+ ANALYZ POWER
C	012	POLARIZATION	EXPT-PROG	79+6		NEANDC(E)-232U	882	IFS		VOL.V.P.57	BULSKI+ ANALYZ POWER
C	012	POLARIZATION	EXPT-PROG	81+6		NEANDC(E)-232U	882	IFS		VOL.V.P.57	BULSKI+ ANALYZ POWER
C	012	POLARIZATION	EXPT-PROG	87+6		NEANDC(E)-232U	882	IFS		VOL.V.P.57	BULSKI+ ANALYZ POWER
C	012	ELASTIC SCAT	EXPT-PROG	FAST		NEANDC(E)-232U	882	PTB		VOL.5.P.70	ALBERTS, TOF EXPT,NDG
C	012	TOTAL	EXPT-PROG	FAST		NEANDC(E)-232U	882	PTB		VOL.5.P.70	ALBERTS, TOF EXPT,NDG
NE	020	N,GAMMA	EXPT-PROG	50+3	20+5	NEANDC(E)-232U	882	KFK		VOL.5.P.1	ALMEIDA. TOF, ABST NDG
NE	021	N,GAMMA	-PROG	50+3	20+5	NEANDC(E)-232U	882	KFK		VOL.5.P.1	ALMEIDA. TOF, ABST NDG
NE	022	N,GAMMA	-PROG	50+3	20+5	NEANDC(E)-232U	882	KFK		VOL.5.P.1	ALMEIDA. TOF, ABST NDG
AL	027	N,TRITON	EXPT-PROG	15+7	20+7	NEANDC(E)-232U	882	JUL		VOL.V.P.26	QAIM+ EXCIT FN, CFD CALC
AL	027	RESON PARAMS	-PROG	35+4		NEANDC(E)-232U	882	KFK		VOL.5.P.1	WISSHAK+ S-WAVE,NDG
SI		N,PROTON	EXPT-PROG	78+6		NEANDC(E)-232U	882	IFS		VOL.V.P.57	BULSKI+PROTON RECOIL SPEC
TI		N,TRITON	EXPT-PROG	30+7		NEANDC(E)-232U	882	JUL		VOL.V.P.26	QAIM+ SIG 0.55MB
V		N,TRITON	EXPT-PROG	30+7		NEANDC(E)-232U	882	JUL		VOL.V.P.26	QAIM+ SIG 0.55MB
MN		N,TRITON	EXPT-PROG	30+7		NEANDC(E)-232U	882	JUL		VOL.V.P.26	QAIM+ SIG 0.55MB
FE		N,TRITON	EXPT-PROG	30+7		NEANDC(E)-232U	882	JUL		VOL.V.P.26	QAIM+ SIG 0.55MB
FE	056	N,GAMMA	-PROG	10+4	25+5	NEANDC(E)-232U	882	KFK		VOL.5.P.2	KAEPPELER+ TOF, ABST,NDG
FE	056	RESON PARAMS	-PROG	10+4	10+5	NEANDC(E)-232U	882	KFK		VOL.5.P.2	KAEPPELER+ RES PARS, NDG
FE	056	RESON PARAMS	-PROG	28+4		NEANDC(E)-232U	882	KFK		VOL.5.P.1	WISSHAK+ , S-WAVE,NDG
FE	058	N,GAMMA	-PROG	10+4	25+5	NEANDC(E)-232U	882	KFK		VOL.5.P.2	KAEPPELER+ TOF, ABST NDG
FE	058	RESON PARAMS	-PROG	10+4	10+5	NEANDC(E)-232U	882	KFK		VOL.5.P.2	KAEPPELER+ RES PARS, NDG
CO	059	N,TRITON	EXPT-PROG	15+7	20+7	NEANDC(E)-232U	882	JUL		VOL.V.P.26	QAIM+ EXCIT FN, CFD CALC
NI	058	N,ALPHA	EXPT-PROG	40+6	90+6	NEANDC(E)-232U	882	JUL		VOL.V.P.26	QAIM+ EXCIT FN,SIG,NDG
NI	058	RESON PARAMS	-PROG	15+4		NEANDC(E)-232U	882	KFK		VOL.5.P.1	WISSHAK+ S-WAVE,NDG
NI	060	RESON PARAMS	-PROG	13+4		NEANDC(E)-232U	882	KFK		VOL.5.P.1	WISSHAK+ S-WAVE,NDG
CU		N,TRITON	EXPT-PROG	30+7		NEANDC(E)-232U	882	JUL		VOL.V.P.26	QAIM+ SIG 0.55MB
CU		POLARIZATION	EXPT-PROG	78+6		NEANDC(E)-232U	882	IFS		VOL.V.P.57	BULSKI+ ANALYZ POWER
ZN		TOTAL	EXPT-PROG	13+0		NEANDC(E)-232U	882	MUN		VOL.5.P.51	KOESTER+ 4.203B
ZN		TOTAL	EXPT-PROG	50-4		NEANDC(E)-232U	882	MUN		VOL.V.P.51	KOESTER+ 7.9B
ZN		TOTAL	EXPT-PROG	52+0		NEANDC(E)-232U	882	MUN		VOL.5.P.51	KOESTER+ 4.114B
ZN		THERMAL SCAT	EXPT-PROG	NDG		NEANDC(E)-232U	882	MUN		VOL.5.P.51	KOESTER+ INCOHERENT SCAT
ZN		THERMAL SCAT	EXPT-PROG	NDG		NEANDC(E)-232U	882	MUN		VOL.V.P.50	KOESTER+ COH SCAT LENGTH
ZN		THERMAL SCAT	EXPT-PROG	00+0		NEANDC(E)-232U	882	MUN		VOL.5.P.51	KOESTER+ 4.06B
ZN		THERMAL SCAT	EXPT-PROG	25-2		NEANDC(E)-232U	882	MUN		VOL.5.P.51	KOESTER+ ABS SIG
ZN	064	THERMAL SCAT	EXPT-PROG	NDG		NEANDC(E)-232U	882	MUN		VOL.V.P.50	KOESTER+ COH SCAT LENGTH
ZN	066	THERMAL SCAT	EXPT-PROG	NDG		NEANDC(E)-232U	882	MUN		VOL.V.P.50	KOESTER+ COH SCAT LENGTH
ZN	067	THERMAL SCAT	EXPT-PROG	NDG		NEANDC(E)-232U	882	MUN		VOL.V.P.50	KOESTER+ COH SCAT LENGTH
ZN	068	THERMAL SCAT	EXPT-PROG	NDG		NEANDC(E)-232U	882	MUN		VOL.V.P.50	KOESTER+ COH SCAT LENGTH
GA		TOTAL	EXPT-PROG	13+0		NEANDC(E)-232U	882	MUN		VOL.5.P.51	KOESTER+ 7.583B
GA		TOTAL	EXPT-PROG	50-4		NEANDC(E)-232U	882	MUN		VOL.5.P.51	KOESTER+ 20.0B
GA		TOTAL	EXPT-PROG	52+0		NEANDC(E)-232U	882	MUN		VOL.5.P.51	KOESTER+ 7.091B
GA		THERMAL SCAT	EXPT-PROG	NDG		NEANDC(E)-232U	882	MUN		VOL.V.P.50	KOESTER+ LIQUID,SCATLENGT
GA		THERMAL SCAT	EXPT-PROG	NDG		NEANDC(E)-232U	882	MUN		VOL.5.P.51	KOESTER+ INCOHERENT SCAT
GA		THERMAL SCAT	EXPT-PROG	00+0		NEANDC(E)-232U	882	MUN		VOL.5.P.51	KOESTER+ 7.03B
GA		THERMAL SCAT	EXPT-PROG	25-2		NEANDC(E)-232U	882	MUN		VOL.5.P.51	KOESTER+ ABS SIG
SE		TOTAL	EXPT-PROG	13+0		NEANDC(E)-232U	882	MUN		VOL.5.P.51	KOESTER+ 9.495B

ELEMENT S	A	QUANTITY	TYPE	ENERGY MIN	ENERGY MAX	DOCUMENTATION REF	VOL	PAGE	DATE	LAB	COMMENTS
SE		TOTAL	EXPT-PROG	52+0		NEANDC(E)-232U	882		MUN	VOL.5.P.51	KOESTER+ 8.295B
KR	080	N,GAMMA	-PROG	MAXW	30+5	NEANDC(E)-232U	882		KFK	VOL.5.P.3	WALTER+ FROM NG-EXPT CALC
KR	080	N,GAMMA	-PROG	40+4	29+5	NEANDC(E)-232U	882		KFK	VOL.5.P.3	WALTER+ TOF REL AU197, NDG
KR	086	N,GAMMA	-PROG	MAXW	30+5	NEANDC(E)-232U	882		KFK	VOL.5.P.3	WALTER+ FROM NG-EXPT CALC
KR	086	N,GAMMA	-PROG	40+4	29+5	NEANDC(E)-232U	882		KFK	VOL.5.P.3	WALTER+ TOF REL AU197, NDG
Y	HYD	THERMAL SCAT	COMP-PROG	NDG		NEANDC(E)-232U	882	THS		VOL.5.P.54	KEINERT. SCAT SIG,NDG
ZR	HYD	TOTAL	EXPT-PROG	50-2	12+0	NEANDC(E)-232U	882		KIL	VOL.V.P.31	PRIESMEYER+ BOUND H SIG
ZR	HYD	THERMAL SCAT	COMP-PROG	NDG		NEANDC(E)-232U	882	THS		VOL.5.P.54	KEINERT. SCAT SIG,NDG
NB	093	N,TRITON	EXPT-PROG	15+7	20+7	NEANDC(E)-232U	882		JUL	VOL.V.P.26	QAIM+ EXCIT FN, CFD CALC
NB	093	TOTAL	EXPT-PROG	FISS		NEANDC(E)-232U	882	PTB		VOL.5.P.69	ALBERTS. CF252 FISS SPEC
MO		N,TRITON	EXPT-PROG	30+7		NEANDC(E)-232U	882		JUL	VOL.V.P.26	QAIM+ SIG 0.55MB
AG		N,TRITON	EXPT-PROG	30+7		NEANDC(E)-232U	882		JUL	VOL.V.P.26	QAIM+ SIG 0.55MB
CD	114	N,GAMMA	-PROG	NDG		NEANDC(E)-232U	882		KFK	VOL.5.P.3	WARD+ ACT EXPT, ABST NDG
CS	133	N,HELIUM3	EXPT-PROG	53+7		NEANDC(E)-232U	882		JUL	VOL.V.P.26	QAIM+ TBC,NDG
ND	146	N,HELIUM3	EXPT-PROG	53+7		NEANDC(E)-232U	882		JUL	VOL.V.P.26	QAIM+ TBC,NDG
HO	165	N,HELIUM3	EXPT-PROG	53+7		NEANDC(E)-232U	882		JUL	VOL.V.P.26	QAIM+ TBC,NDG
YB		THERMAL SCAT	EXPT-PROG	NDG		NEANDC(E)-232U	882		MUN	VOL.V.P.50	KOESTER+ COH SCAT LENGTH
YB	170	N,GAMMA	-PROG	30+5		NEANDC(E)-232U	882		KFK	VOL.5.P.4	BEER+ 766MB, ABST
YB	170	THERMAL SCAT	EXPT-PROG	NDG		NEANDC(E)-232U	882		MUN	VOL.V.P.50	KOESTER+ COH SCAT LENGTH
YB	171	THERMAL SCAT	EXPT-PROG	NDG		NEANDC(E)-232U	882		MUN	VOL.V.P.50	KOESTER+ COH SCAT LENGTH
YB	172	THERMAL SCAT	EXPT-PROG	NDG		NEANDC(E)-232U	882		MUN	VOL.V.P.50	KOESTER+ COH SCAT LENGTH
YB	173	THERMAL SCAT	EXPT-PROG	NDG		NEANDC(E)-232U	882		MUN	VOL.V.P.50	KOESTER+ COH SCAT LENGTH
YB	174	N,HELIUM3	EXPT-PROG	53+7		NEANDC(E)-232U	882		JUL	VOL.V.P.26	QAIM+ TBC,NDG
YB	174	THERMAL SCAT	EXPT-PROG	NDG		NEANDC(E)-232U	882		MUN	VOL.V.P.50	KOESTER+ COH SCAT LENGTH
YB	176	THERMAL SCAT	EXPT-PROG	NDG		NEANDC(E)-232U	882		MUN	VOL.V.P.50	KOESTER+ COH SCAT LENGTH
LU	175	N,GAMMA	-PROG	30+5		NEANDC(E)-232U	882		KFK	VOL.5.P.4	BEER+ 1266MB, ABST
HF	178	N,GAMMA	-PROG	26+3	20+6	NEANDC(E)-232U	882		KFK	VOL.5.P.5	BEER+ ABST NDG
HF	179	N,GAMMA	-PROG	26+3	20+6	NEANDC(E)-232U	882		KFK	VOL.5.P.5	BEER+ ABST NDG
HF	179	N,GAMMA	EXPT-PROG	25+4		NEANDC(E)-232U	882		KFK	VOL.5.P.5	BEER+ ABST, 13.5MB
HF	180	N,GAMMA	EXPT-PROG	FAST		NEANDC(E)-232U	882		KFK	VOL.5.P.6	BEER+ ABST NDG
HF	180	N,GAMMA	EXPT-PROG	26+3	20+6	NEANDC(E)-232U	882		KFK	VOL.5.P.5	BEER+ ABST NDG
TA		N,TRITON	EXPT-PROG	30+7		NEANDC(E)-232U	882		JUL	VOL.V.P.26	QAIM+ SIG 0.55MB
TA	180	N,GAMMA	-PROG	26+3	20+6	NEANDC(E)-232U	882		KFK	VOL.5.P.5	BEER+ ABST NDG
W	184	N,GAMMA	EXPT-PROG	FAST		NEANDC(E)-232U	882		KFK	VOL.5.P.6	BEER+ ABST NDG
W	186	N,HELIUM3	EXPT-PROG	53+7		NEANDC(E)-232U	882		JUL	VOL.V.P.26	QAIM+ TBC,NDG
AU	197	N,HELIUM3	EXPT-PROG	53+7		NEANDC(E)-232U	882		JUL	VOL.V.P.26	QAIM+ TBC,NDG
TL		N,TRITON	EXPT-PROG	30+7		NEANDC(E)-232U	882		JUL	VOL.V.P.26	QAIM+ SIG 0.55MB
TL		TOTAL	EXPT-PROG	13+0		NEANDC(E)-232U	882		MUN	VOL.5.P.51	KOESTER+ 10.50B
TL		TOTAL	EXPT-PROG	53+0		NEANDC(E)-232U	882		MUN	VOL.5.P.51	KOESTER+ 10.24B
TL		THERMAL SCAT	EXPT-PROG	NDG		NEANDC(E)-232U	882		MUN	VOL.V.P.50	KOESTER+ LIQUID,SCATLENGT
TL		THERMAL SCAT	EXPT-PROG	NDG		NEANDC(E)-232U	882		MUN	VOL.5.P.51	KOESTER+ INCOHERENT SCAT
TL		THERMAL SCAT	EXPT-PROG	00+0		NEANDC(E)-232U	882		MUN	VOL.5.P.51	KOESTER+ 10.01B
PB		N,TRITON	EXPT-PROG	30+7		NEANDC(E)-232U	882		JUL	VOL.V.P.26	QAIM+ SIG 0.55MB
PB		POLARIZATION	EXPT-PROG	78+6		NEANDC(E)-232U	882		IFS	VOL.V.P.57	BULSKI+ ANALYZ POWER
BI		N,TRITON	EXPT-PROG	30+7		NEANDC(E)-232U	882		JUL	VOL.V.P.26	QAIM+ SIG 0.55MB
BI	209	DIFF ELASTIC	EXPT-PROG	78+6		NEANDC(E)-232U	882		IFS	VOL.V.P.57	BULSKI+ ANGDIST
BI	209	POLARIZATION	EXPT-PROG	78+6		NEANDC(E)-232U	882		IFS	VOL.V.P.57	BULSKI+ ANALYZ POWER
U	235	FISS PROD G	EXPT-PROG	PILE		NEANDC(E)-232U	882		MNZ	VOL.V.P.46	SOHNIUS+ CS+BA 142-143
U	235	STRNTH FNCTN	EXPT-PROG	00+0	10+2	NEANDC(E)-232U	882		KFK	VOL.5.P.19	FROEHNER. S-WAVE
U	238	SPECT N,GAMT	THEO-PROG	+3	+5	NEANDC(E)-232U	882		KFK	VOL.5.P.6	REFFO OPTMDL,STATMDL, ABST
U	238	STRNTH FNCTN	EXPT-PROG	00+0	40+3	NEANDC(E)-232U	882		KFK	VOL.5.P.19	FROEHNER. S-WAVE
PU	239	STRNTH FNCTN	EXPT-PROG	00+0	66+2	NEANDC(E)-232U	882		KFK	VOL.5.P.19	FROEHNER. S-WAVE
PU	240	SPECT N,GAMT	THEO-PROG	+3	+5	NEANDC(E)-232U	882		KFK	VOL.5.P.6	REFFO OPTMDL,STATMDL, ABST
PU	240	STRNTH FNCTN	EXPT-PROG	00+0	30+3	NEANDC(E)-232U	882		KFK	VOL.5.P.19	FROEHNER. S-WAVE
PU	241	STRNTH FNCTN	EXPT-PROG	00+0	16+2	NEANDC(E)-232U	882		KFK	VOL.5.P.19	FROEHNER. S-WAVE
PU	242	SPECT N,GAMT	THEO-PROG	+3	+5	NEANDC(E)-232U	882		KFK	VOL.5.P.6	REFFO OPTMDL,STATMDL, ABST
PU	242	STRNTH FNCTN	EXPT-PROG	00+0	50+2	NEANDC(E)-232U	882		KFK	VOL.5.P.19	FROEHNER. S-WAVE
AM	241	RESON PARAMS	EXPT-PROG	NDG		NEANDC(E)-232U	882		KFK	VOL.5.P.23	GOEL. VS CD-CUTOFF E,GRPH

ELEMENT S A	QUANTITY	TYPE	ENERGY MIN	ENERGY MAX	DOCUMENTATION REF	VOL	PAGE	DATE	LAB	COMMENTS
AM 241	RESON PARAMS	EXPT-PROG	NDG		NEANDC(E)-232U	882	KFK	VOL.V.P.23	GOEL.	VS CD-CUTOFF E,GRPH
AM 241	TOTAL	THEO-PROG	10+4	10+7	NEANDC(E)-232U	882	KFK	VOL.5.P.21	GOEL+	OPTMDL,GRPH
AM 242	N,GAMMA	THEO-PROG	10+3	10+7	NEANDC(E)-232U	882	KFK	VOL.5.P.21	GOEL+	OPTMDL,GRPH
AM 243	EVALUATION	EVAL-PROG	NDG		NEANDC(E)-232U	882	KFK	VOL.5.P.21	GOEL+	NDG
AM 243	N,GAMMA	EXPT-PROG	10+4	25+5	NEANDC(E)-232U	882	KFK	VOL.5.P.7	WISSHAK+	ABST NDG
CM 244	EVALUATION	EVAL-PROG	NDG		NEANDC(E)-232U	882	KFK	VOL.5.P.21	GOEL+	NDG
CF 252	SPECT FISS N	EXPT-PROG	SPON		NEANDC(E)-232U	882	PTB	VOL.5.P.71	BOETTGER+	NDG